VOLUME 21, 1959/60, No. 10 pp. 281-316 Published 30th August 1960

Philips Technical Review

DEALING WITH TECHNICAL PROBLEMS
RELATING TO THE PRODUCTS, PROCESSES AND INVESTIGATIONS OF
THE PHILIPS INDUSTRIES

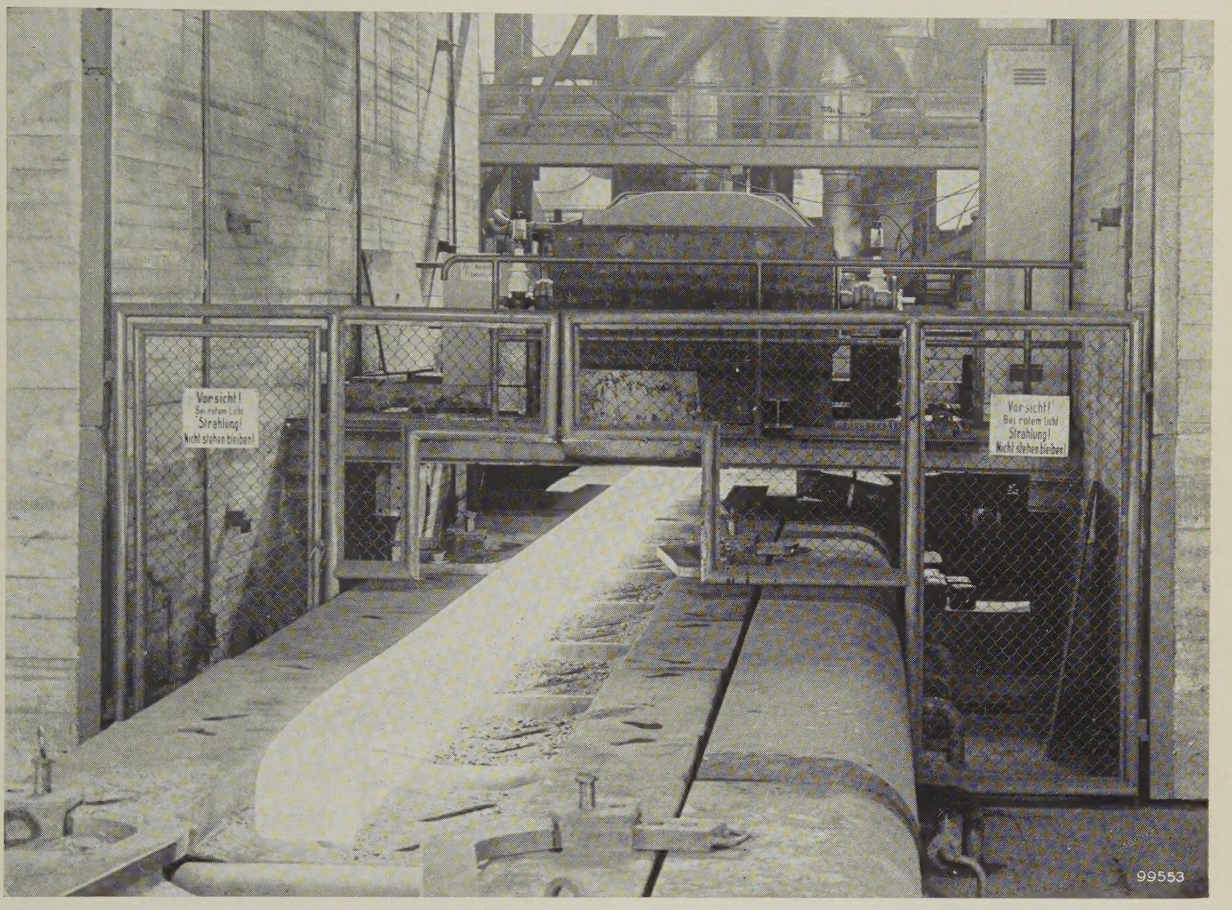

X-RAY INSPECTION OF HOT STEEL BILLETS DURING ROLLING

by W. J. OOSTERKAMP, J. PROPER and M. C. TEVES. 620.179.152:621.771

In teelworks the molten steel prepared in open-hearth furnaces, Bessemer converters or electric furnaces is cast in iron moulds, in which it solidifies into ingots of several tons. After the ingots have set, but before further cooling, they are taken from the moulds and reduced in a roughing mill to billets or blooms about thirty feet long and $8'' \times 8''$ or more in cross-section. Frequently the billets are immediately subjected to further rolling operations to reduce them to bars or sections only an inch or so thick.

A problem encountered in this process is that blowholes are formed in the steel during solidification, which, if not plugged by the rolling, materially weaken the finished product. The same applies to slag inclusions in the steel. Experience has shown that defects of this kind are particularly prevalent in the front end (the "crop") of the billet, and it is therefore the invariable practice to cut off an end portion some metres in length and to discard it as scrap. Inspection of the cut face for holes or inclusions reveals whether too much or too little has been discarded. The presence of such defects, however, cannot be very clearly observed on the red-hot metal. Consequently it is quite possible that

in fact too little will be removed, which means that poor-quality steel is passed for further processing, or that, to be on the safe side, too much is cut off, which is a waste of good material.

It is evident that X-ray investigation of the hot billets in the rolling mill would result in a considerable saving of material and also make for a more reliable product. Furthermore, it would show whether defects were present in parts of the billet other than the crop, and finally — and this is perhaps the most important point — it would provide a practical and simple means of investigating the effect of various production factors on the formation of cavities and other casting defects. It was indeed similar considerations that led to the widespread adoption of X-radiography for the inspection of welds; apart from its great utility for routine inspections, radiography has also contributed substantially to the improvement of welding techniques [1]).

In the present case it is a matter of detecting holes or inclusions, measuring only a few millimetres across, in a steel billet at least 200 mm ($\sim 8''$) thick, and which, moreover, is moving at a steady rate of, say, a foot or two per second. For this purpose the normal X-ray equipment for industrial radiography, using X-radiation up to 300 keV, is hopelessly inadequate: the half-value layer of steel for X-ray energies of 300 keV is 6.5 mm, which means that this radiation is attenuated in steel 200 mm thick by a factor of about 2^{-30} or 10^{-9}!

At the steelworks of Phoenix-Rheinrohr AG, Düsseldorf, plans were developed to tackle this problem with the aid of various modern devices: a betatron as radiation source, an X-ray image intensifier as detector and an industrial closed-circuit television system for the final display. Preliminary tests and investigations, for which Philips made available a special X-ray image intensifier (designed for other purposes), led to the conclusion that the envisaged equipment would meet the requirements. One of the rolling plants at Phoenix-Rheinrohr was then equipped with a trial installation, and several thousand hot billets were subjected to X-ray fluoroscopy. Some particulars of this installation and of the results obtained are given below [2]).

The betatron radiation source, a product of Brown Boveri (Switzerland), generates X-ray energies up to 31 MeV. This extremely hard radiation can be used for fluoroscopy of relatively very thick materials, especially since the betatron gives an appreciable intensity, comparable to that of an X-ray tube working on 300 kV, 10 mA. What is more, an X-ray energy in the region of 30 million electronvolts is about the most favourable that can be chosen in this case, the penetrating power in steel then being greatest; at higher energies the absorption in steel progressively increases as a result of pair production. Nevertheless, the half-value layer of steel for 31 MeV radiation is only 34 mm, which is still much smaller than the object thickness. After traversing 200 mm of steel, the rays are reduced in intensity to about 2^{-6}, i.e. to roughly 1% of the initial value. Observation at this low residual intensity is made possible by the X-ray image intensifier, to which we shall refer presently. The third part of the installation is, as mentioned above, an industrial television system for remote display of the image formed on the viewing screen of the image-intensifier tube. This television equipment uses an image-orthicon camera tube and was supplied by Fernseh GmbH of Darmstadt. A full-size image of the viewing screen is formed in the usual way on the photocathode of the image orthicon by a conventional optical system. The use of television offers several advantages. In the first place it is the easiest answer to the problem of safely positioning the observer, who cannot of course be immediately behind the intensifier viewing screen, where the level of residual radiation is still dangerously high. Further, the television system, with its extremely sensitive image orthicon, enables a luminance gain to be obtained that supplements that of the image intensifier. Finally, it is a simple matter in a television circuit to provide for *contrast intensification* [3]). All these favourable factors make it possible in the installation described to achieve better detail perceptibility than if the viewing screen were observed by means of mirrors and a telescope — a method which, although safe for the observer, is hardly a reasonable proposition in a steel-rolling plant.

Since a uniform brightness is obtained in the whole field of view during the screening of the rectangular-sectioned steel billets, a considerable degree of contrast intensification may be applied. To obtain a uniform intensity distribution across the X-ray beam from the betatron, a suitably shaped equalizing absorber is placed in front of the betatron window.

---

[1]) An alternative and widely used method of non-destructive testing is by means of ultrasonic vibrations; this is not suitable for examining hot billets, however, because of excessive damping in the material at the temperatures involved.

[2]) For a detailed report see W. Lückerath, K. Fink and R. Flossmann, Stahl und Eisen **79**, 1637, 1959 (No. 22).

[3]) Contrast control, but usually with the object of attenuating instead of intensifying contrast, is common practice in television, a gamma corrector circuit being used for the purpose. See e.g. Philips tech. Rev. **15**, 227 *et seq.*, 1953/54. The circuit there employed permits a contrast gain of up to 1.5×. Other circuits are used for obtaining the much higher contrast intensification required in the present case.

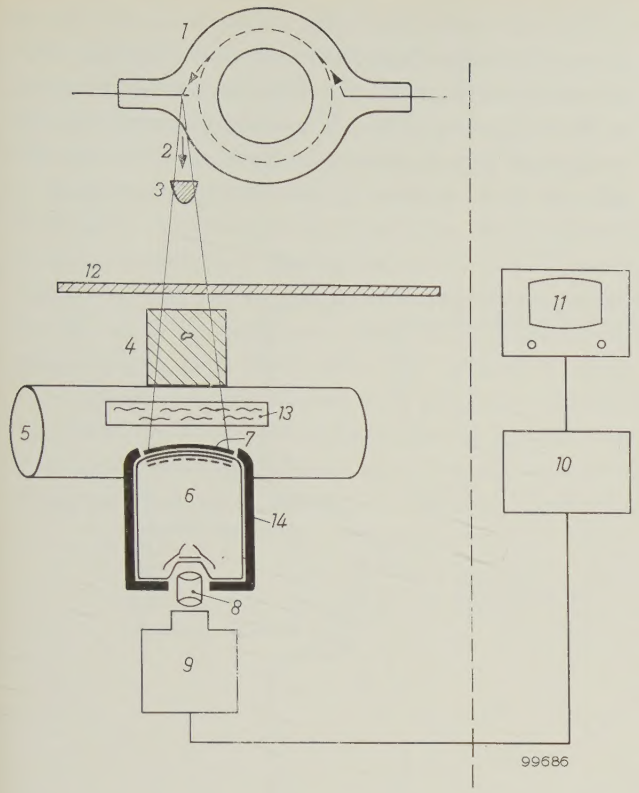

Fig. 1. Schematic cross-section of the trial installation at Phoenix-Rheinrohr, Düsseldorf, for visual X-ray inspection of hot steel billets during rolling. *1* betatron tube. *2* beam of 31 MeV X-rays. *3* copper equalizing absorber. *4* steel billet, which moves along a line of rollers *5* under the betatron. *6* X-ray image intensifier tube with lead layer *7* over aluminium window. *8* optical system. *9* television camera tube. *10* television video circuits. *11* display tube. *12* aluminium plate which shields the betatron from the heat radiated by the hot steel. *13* water-cooled heat-radiation shield for the image-intensifier tube. *14* lead shield to prevent scattered X-rays from penetrating into the image intensifier.

The layout of the installation is illustrated in *figs. 1* and *2*, and some additional details are mentioned in the captions.

The X-ray image intensifier works on the principle described in previous articles in this journal. X-rays falling on a fluorescent screen excite an image, the photons of which release electrons from a photocathode in contact with this fluorescent screen. These electrons are accelerated by a high potential (25 kV) and focused on a second fluorescent screen, the viewing screen. The image intensifier placed at the disposal of Phoenix-Rheinrohr (see *fig. 3*) had a tube wall made entirely of aluminium and gave an electron-optical reduction of more than 10 times, and an overall luminance gain of about 1200 times. The field of the image intensifier, i.e. the diameter of the X-ray fluorescent screen, is 9″; this is the same as that of the recently introduced image intensifier for medical applications. It is thus an intermediate size between the types earlier described, of 5″ and 11″ [4]). For use in conjunction with the betatron, a layer of lead 2 mm thick was fitted over the aluminium window of the intensifier. This was done

[4]) M. C. Teves and T. Tol, Electronic intensification of fluoroscopic images, Philips tech. Rev. **14**, 33-43, 1952/53 (description of 5″ tube). The 11″ tube is described in Philips tech. Rev. **20**, 331-345, 1958/59 (No. 11).

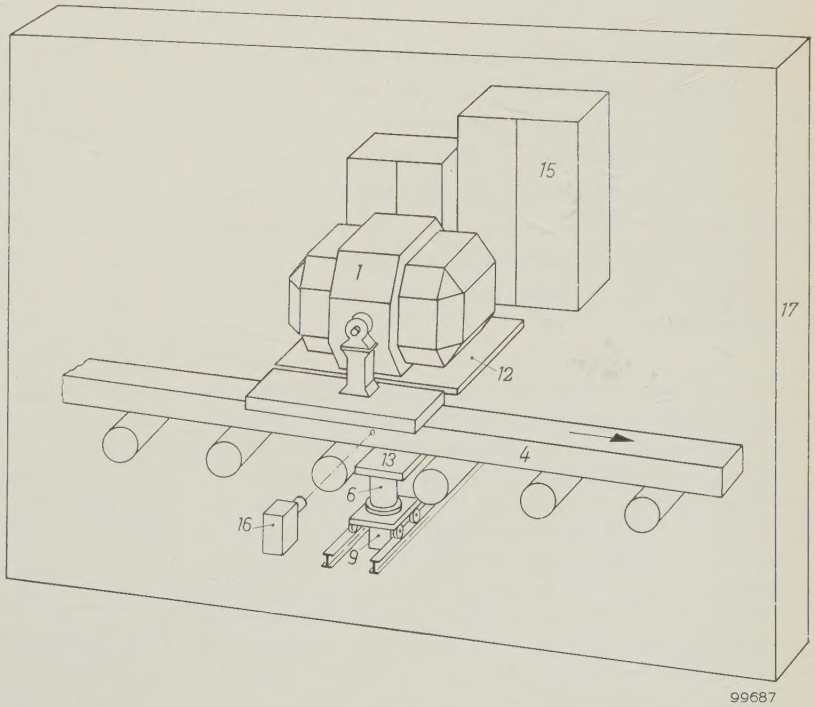

Fig. 2. Perspective sketch of the installation. Meaning of numbers as in fig. 1. Other numbers: *15* power pack for betatron. *16* second television camera, enabling observer to keep an eye on the movement of the billet. *17* one of the concrete walls that help to shield the environment against X-radiation scattered from the billet (see also title photograph). The image intensifier *6* and the camera tube *9* are mounted on a carriage to permit lateral displacement.

because only a very small fraction of the 31 MeV radiation is directly absorbed by the X-ray screen and used for producing the fluorescent light. In the lead, the 31 MeV X-rays release electrons that possess an energy of about 10 MeV and travel in directions not very different from the beam of X-rays.

The extremely high gain obtained in the X-ray image intensifier (and in the television circuit) does not alter the fact that the information, upon arrival in the image intensifier, is carried by a relatively low number of X-ray quanta. A high "noise" level in the picture is therefore inevitable [5]). The effect is

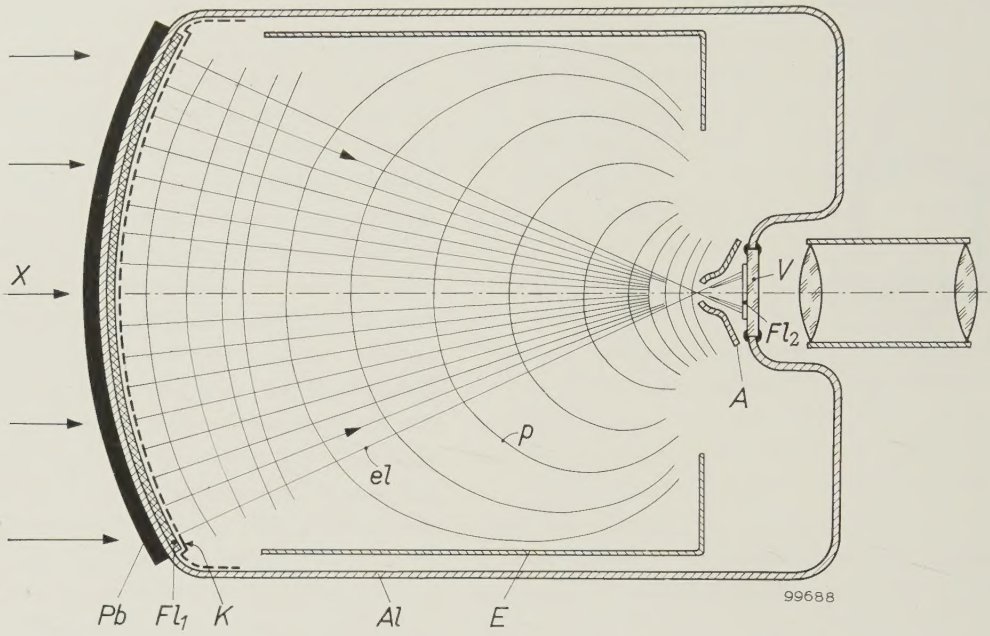

Fig. 3. Cross-section of the Philips 9″ X-ray image intensifier placed at the disposal of Phoenix-Rheinrohr AG. *Al* aluminium wall of tube. Fl_1 X-ray screen. *K* photocathode. *E* focusing electrode. *A* anode. Fl_2 viewing screen. *V* glass viewing window. A number of electron paths (*el*) and the cross-sections of a number of equipotential surfaces (*p*) are shown. For the purpose of the experiment a lead layer *Pb* was fitted over the aluminium wall covering the X-ray screen: the incident 31 MeV X-radiation (*X*) releases electrons from this layer.

These electrons pass through the aluminium window without appreciable scattering (the window is only 1 mm thick) and in the fluorescent screen, fitted on the inside of the window, they excite about 4000 photons of fluorescent light per electron. Image intensification then occurs as already outlined above, and each 10 MeV electron from the lead gives rise finally to 400 000 light photons from the viewing screen.

It is worth pausing here to reflect on the remarkable sequence of particle interactions occurring in this equipment. *Electrons*, accelerated in the betatron, generate *X-ray photons* in the target, and these, after passing through the object, liberate in their turn *electrons* from the lead shield. These strike the X-ray screen, where they excite *light photons*, which again release *electrons* from the photocathode. These electrons, after acceleration, finally produce *light photons* again in the viewing screen. In the television system there is the further sequence of electronic phenomena by which the picture information is transmitted to the picture tube, where it is again converted to light photons that finally reach the eye of the observer.

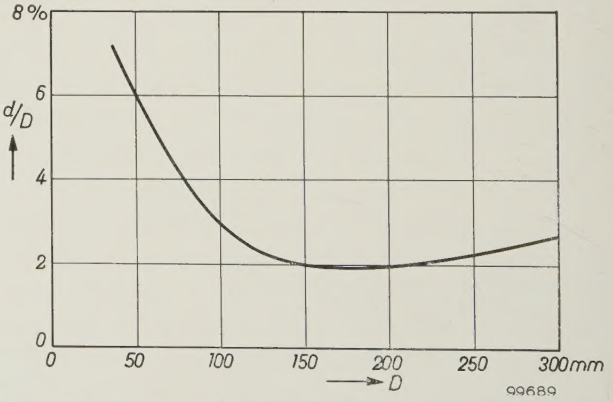

Fig. 4. Perceptibility of thin wires on a steel billet (penetrameter test) during inspection with the installation described. The percentage thickness (d/D) of the thinnest wire still just perceptible is plotted as a function of the thickness D of the steel.

[5]) For a more detailed consideration of noise in X-ray images see: T. Tol and W. J. Oosterkamp, The application of the X-ray image intensifier, II. The perception of small object-detail, Philips tech. Rev. **17**, 71-77, 1955/56.

reduced to some extent by the afterglow of the television picture tube, in which each image element is integrated over a certain time. Of course, the afterglow persistence may not be unduly long in view of the fact that the steel billet is a moving object.

In spite of the remaining noise, the trial installation gave surprisingly good results. Penetrameter measurements (i.e. determination of the thinnest wires still just perceptible) yielded the curve shown in *fig. 4*. This indicates that, in a fluoroscopic examination of a steel billet 200 mm (8″) thick, steel wires of 4 mm diameter on the billet can still be observed. A statistical analysis was made of the casting defects found during the screening of several thousand hot steel billets at Phoenix-Rheinrohr, against the defects found during the subsequent inspection of cold sawn-off sections. The conclusion was that screening in this way discloses 50% of all blowholes 3 mm thick and 90% of all blowholes 7 mm thick.

Summary. In steelworks the quality of the finished product can be improved and needless waste of material avoided if the presence of blowholes and inclusions can be detected *during* the rolling of the hot billets (cross-section of the order of 8″×8″). To this end a trial installation was designed and constructed by Phoenix-Rheinrohr AG, Düsseldorf, in which the steel billets were moved through a beam of 31 MeV X-rays generated in a betatron, and the image observed with the aid of a special X-ray image intensifier (field of 9″ diameter) and an industrial television system. The results of screening several thousand hot billets showed that 50% of all holes 3 mm thick where detected, and 90% of all holes 7 mm thick.

NUCLEAR MAGNETIC RESONANCE

by D. J. KROON.

539.143.42.082.722.56:620.18

The phenomenon of nuclear magnetic resonance in solids and liquids yields absorption spectra from which valuable information on their structures can be obtained. The article below first gives a simple exposition of the theory, and then describes in more detail the equipment required and a few applications. The latter illustrate the usefulness of the method both for pure scientific research and for routine investigations in various industries.

Introduction

Amongst the most recent tools in the investigation of condensed phases (solids and liquids) are the methods of measurement that depend on the absorption of electromagnetic energy at specific wavelengths in the metre and centimetre regions. According to the mechanism causing the absorption, the methods can be divided into three groups: paramagnetic resonance, nuclear magnetic resonance and cyclotron resonance.

In paramagnetic and nuclear magnetic resonance the absorption is caused by the presence in the substance of elementary magnets, i.e. the "spins" of electrons and atomic nuclei which, in the presence of a constant external magnetic field, are subjected to an *alternating magnetic* field. Cyclotron resonance occurs when more or less free electrons (e.g. in semiconductors), in the presence of a constant external magnetic field, are subjected to an alternating *electric* field. In this article we shall be concerned only with nuclear magnetic resonance. The related effect of paramagnetic resonance was described in an article published some time ago in this journal [1]), to which we shall refer when occasion arises. An appendix to the present article deals in some detail with the points of difference between paramagnetic and nuclear magnetic resonance.

As mentioned, nuclear magnetic resonance occurs when atomic nuclei exhibit a spin, that is to say, they have a net angular momentum and magnetic moment. This is so with many kinds of nuclei, in principle in all cases where the number of neutrons and the number of protons in the nucleus are not both even. Familiar examples of nuclei that show a readily measurable effect, i.e. a marked absorption, are ^{19}F, ^{23}Na, ^{27}Al and ^{31}P, but most especially ^{1}H, the hydrogen nucleus or proton.

The information that nuclear magnetic resonance can provide is of various kinds. Hydrogen atoms are present in many inorganic solids (e.g. in molecules of water of crystallization) and in nearly all organic molecules. The form in which the hydrogen nuclei are present has an influence on the resonance spectrum, i.e. the spectral distribution of the measured absorption. In an organic liquid, for example, each kind of molecule containing hydrogen shows a characteristic line spectrum, which can therefore serve for identifying the molecule. In this way it is possible to analyse mixtures of organic compounds. Nuclear magnetic resonance equipment is for this reason regularly used for routine analyses in the petroleum and oil-refining industries and the plastics industry. In solids the resonance frequency of the H nucleus is very broad. From the spectral distribution of the absorption here, one can draw conclusions regarding the ordering of H ions and other ions in the crystal and also regarding the motion of electrons and ions, diffusion phenomena, and so on.

An earlier article in this Review explained how nuclear magnetic resonance can also be used for the accurate measurement of magnetic fields [2]). We shall touch on this application when describing the equipment.

In the following pages we shall first give a simple theory of the phenomenon of nuclear magnetic resonance. After describing the measuring equipment we shall consider, by way of illustration, some examples of problems that have been studied by the method of nuclear magnetic resonance. When dealing with the equipment we shall distinguish between measurements on solids and on liquids. Owing to the different nature of their spectra, these two states of aggregation call for different techniques of measurement.

For the determination of crystal structures the well-established methods of X-ray diffraction and infra-red absorption can also be used. It is important to note, however,

[1]) J. S. van Wieringen, Paramagnetic resonance, Philips tech. Rev. **19**, 301-313, 1957/58.

[2]) H. G. Beljers, Three methods of measuring magnetic fields, III. Measurement by the proton-resonance method, Philips tech. Rev. **15**, 55-62, 1953/54.

that these methods are not so suitable when it is a matter of detecting and localizing hydrogen atoms.

X-ray diffraction depends on the scattering of X-rays by the atoms or ions of which a crystal lattice is built up. This scattering decreases rapidly the lower the atomic number of the atom or ion. Scattering by H ions is so weak that information on these ions can be obtained from X-ray-diffraction measurements only by indirect means. The related method of neutron diffraction is better in this respect, and in fact has proved very useful [3]). It can only be adopted, however, in laboratories associated with a suitable nuclear reactor. Moreover, in these investigations it is often desirable to replace the hydrogen ions (protons) by ions of heavy hydrogen (deuterons), which of course is only practicable in special cases [4]).

The infra-red absorption of hydrogen atoms bound to oxygen (OH vibrations) is readily measurable. The frequency of these vibrations depends markedly on the surroundings of the OH group in the lattice, and it is frequently possible to deduce the configurations in which the OH group occurs in the crystal. The interpretation of the measurements, however, is very complicated and the information obtained is generally insufficient for a complete determination of the structure. Furthermore, the sample under measurement is required to be transparent to some extent, which often calls for the use of special techniques.

The method of nuclear magnetic resonance is thus a useful complement to the older methods of structure determination

Historical note

As long ago as 1936 the Dutch physicist C. J Gorter predicted the possibility that electromagnetic waves would be absorbed in a solid through the agency of the atomic nuclei if these were subjected to an external magnetic field. His experiments at the time produced no results. It later appeared that the substances on which the experiments were done happened to show only a very small effect, and this was the main reason for the failure of the experiment. Some years later, thanks to the advances in high-frequency techniques, the physicists F. Bloch and E. M. Purcell, working independently and with different methods of measurement, were able to confirm Gorter's theory. In 1952 both these American workers were awarded the Nobel prize for physics.

Concise formulation of the theory of nuclear magnetic resonance

In general an atomic nucleus possesses, apart from mass and electric charge, an angular momentum and a magnetic moment. In the classical model, the atomic nucleus is imagined to behave like a rapidly spinning magnetic top, the magnetization being in the direction of the axis of rotation. Quantum-mechanical considerations require that if the nucleus be subjected to a constant external magnetic field, the axis of rotation of the top, which precesses about the field direction, can assume only certain discrete orientations with respect to the direction of the magnetic field. The number of possible orientations depends on the magnitude of the angular momentum. For hydrogen nuclei (protons) there are two possible orientations, viz. in the direction of the field and opposite thereto. Other nuclei have two or more possible orientations (fluorine 2, sodium 4, bismuth 10).

The energy of the nuclear magnet in the magnetic field is:

$$E = \mu B \cos \vartheta,$$

where μ is the magnitude of the magnetic moment, B the field strength (induction) and ϑ the angle between the elementary magnet and the external field (*fig. 1*). The possible values of cos ϑ are given by the formula:

$$\cos \vartheta = \frac{m_I}{\sqrt{I(I+1)}},$$

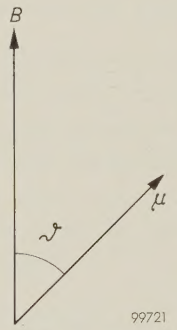

Fig. 1. Magnetic dipole (moment μ) in a magnetic field B.

where I, the spin quantum number of the nucleus, is a multiple of $\frac{1}{2}$, and m_I can assume a number $(2I+1)$ of discrete values, each differing by 1, the extremes being I and $-I$. The energy E can also be written in the form:

$$E = \mu_z B \frac{m_I}{I},$$

where $\mu_z = \mu\sqrt{I/(I+1)}$ represents the largest possible projection of μ on the axis of the field. The magnetic moment μ is given by:

$$\mu = g\sqrt{I(I+1)}\,\frac{e\,h}{4\pi m_p}, \quad \ldots . \quad (1)$$

where e and m_p represent respectively the charge and mass of the proton, and g is a numerical constant

[3]) G. E. Bacon, Neutron diffraction, Oxford Univ. Press, London 1955. See also G. E. Bacon, Ned. T. Natuurk. **25**, 5, 1959 (No. 1).

[4]) G. R. Ringo, Neutron diffraction and interference, Section 36, Handb. Physik, Vol. **32**, Springer, Berlin 1957, p. 603. J. A. Goedkoop and B. O. Loopstra, Ned. T. Natuurk. **25**, 29, 1959 (No. 2).

that differs according to the type of nucleus (in general g is between 0.1 and 10).

The spin quantum number for hydrogen nuclei is $I = \frac{1}{2}$. There are thus, as remarked, only two states possible. The energy difference between these states is

$$\Delta E = 2\mu_z B. \quad \ldots\ldots \quad (2)$$

In an external field $B = 0.5$ Wb/m^2 [5000 gauss] this energy difference is of the order of 10^{-26} J (10^{-7} electronvolt).

If the nucleus is subjected simultaneously to a constant magnetic field and an alternating magnetic field at right angles thereto, there is a possibility that the atomic nucleus will change from the one state to the other, whereby an amount of energy equal to the difference ΔE will be absorbed from the alternating field or given up to it. The condition for the occurrence of such transitions is that the frequency f of the alternating field should satisfy:

$$f = \frac{\Delta E}{h}, \quad \ldots\ldots \quad (3)$$

where h is Planck's constant ($h = 6.62 \times 10^{-34}$ Js).

Eliminating ΔE from the expressions (2) and (3) gives the condition for resonance absorption as

$$f = \frac{2\mu_z}{h} B, \quad \ldots\ldots \quad (4a)$$

or, after substitution of μ_z (from (1)) and putting $I = \frac{1}{2}$:

$$f = g \frac{e}{4\pi m_p} B. \quad \ldots\ldots \quad (4b)$$

For hydrogen nuclei μ_z is 1.4×10^{-26} A.m^2. In a field of $B = 0.5$ Wb/m^2, as mentioned above, we thus have $f = 21.3$ Mc/s.

The procedure for observing the absorption is basically as follows. A sample of the substance having sufficient nuclei of the type under investigation is introduced into a coil which is connected to a weak high-frequency source of roughly the resonance frequency f_0. The coil is placed between the poles of a magnet and the magnetic field is slowly varied. When the magnetic field B_0 reaches the value given by (4a) — for the frequency f_0 — resonance occurs, giving rise to a slight energy absorption which results in a change in the Q of the coil. By including the latter in a suitable circuit, e.g. a bridge circuit, the change in the Q can be measured and recorded as a function of B, to give the magnetic absorption spectrum. The effect of relaxation phenomena on the absorption will be touched on presently.

Structure of the absorption spectrum

From the mechanism described it might be inferred that resonance absorption occurs only at a single frequency, determined by (4a) or, if the frequency f_0 is given, at a certain induction B_0, given by:

$$B_0 = \frac{h}{2\mu_z} f_0.$$

The experiment shows, however, that absorption occurs in a certain region of B values around B_0, and that the recorded absorption line thus has a certain width, and sometimes a certain structure. This may partly be attributed to the fact that, whereas a field B has been applied and measured, the nuclei investigated may in reality be in a field that differs from B by a small amount b. The resonance condition is then:

$$B + b = \frac{h}{2\mu_z} f_0 = B_0,$$

or

$$B = B_0 - b.$$

Absorption thus occurs at a value B of the measuring field that differs from B_0. If b differs for various parts of the specimen or for various kinds of nucleus, the result is a broadened line or a line spectrum. One may also conceive of performing the experiment such that the external field (B_0) is kept constant and the frequency f varied. In that case resonance would occur when $f = f_0 + \Delta f = (2\mu_z/h)(B_0 + b)$, so that $\Delta f = (2\mu_z/h)b$. The value $\Delta f = 1$ c/s corresponds to $b = 2 \times 10^{-8}$ Wb/m^2.

Various reasons can be given for the occurrence of the field-strength deviations b. The first is quite trivial, being of an instrumental nature and connected with the fact that the magnetic field is not perfectly uniform. As a result, parts of the specimen are found in a field that is not exactly identical with the field B. This source of broadening can be reduced to negligible proportions by using small specimens and a magnet whose air gap is narrow compared with the diameter of the pole pieces. This applies at least to solids in which, for other reasons (to be discussed), marked broadening effects occur in any case. In liquids, which generally exhibit a spectrum having sharp resonance lines, the instrumental broadening may not be negligible.

Another cause of instrumental broadening is found especially when recording the spectra of solids. As we shall see, in such cases the measurement is performed by finding an average value over a range δB of field strengths. Since δB cannot be

made infinitely small, this also gives rise to line broadening (see later, fig. 10*a*).

The other causes of line broadening and of the occurrence of line spectra, discussed in the following, are essentially concerned with the physical conditions to which the nuclei are subject during the experiment, and about which the absorption spectrum can therefore provide information.

Local fields in crystals

For the present we shall confine the discussion to solids, that is to crystals. In a crystal the field acting on the nuclei consists of the external field B (now assumed to be uniform) together with the dipole fields of neighbouring nuclei. For hydrogen nuclei this dipole field at a distance of 1 Å is of the order of 10^{-3} Wb/m^2. The total field acting on a nucleus subjected to a dipole field b is $B + b$. At resonance we again have $B + b = B_0$, hence:

$$B = B_0 - b.$$

The resonance line is then (in terms of B) displaced over a distance b.

A case frequently encountered is that of two neighbouring protons. This is found when investigating the absorption of two protons of a molecule of water of crystallization (H-O-H). The field b caused by the one proton at the position of the other depends on the distance r between the two protons and on the angle ϑ which the line connecting them makes with the external field B. The dipole field is given by:

$$b = \pm \frac{\mu_z}{r^3}(3\cos^2\vartheta - 1). \quad . \; . \; . \quad (5)$$

The $\pm$ sign arises because the "perturbing" proton can be oriented in two ways in the field B. For one pair of protons we then obtain, instead of a single resonance peak, two peaks at a distance $2b$ apart. We shall see presently that, as regards the magnitude of the effect, this statement requires some modification.

This, then, is the situation when we have a single crystal and consider the proton pairs therein which take up a specific orientation with respect to the crystal axes. If we turn from a single crystal to a powder, we find that the angle ϑ for the kind of proton pairs considered has a different value in each crystallite of the powder. The resonance pattern is consequently smeared out to a broad band in which, however, two peaks can still be recognized.

So far our discussion has taken account only of neighbouring protons forming a particular H-H pair, for example the protons of a single H-O-H molecule. These protons will also, however, be subjected to the dipole fields of protons of other H-O-H molecules and in addition to the dipole fields of other crystal nuclei. This causes a further broadening of the absorption pattern. As an example *fig. 2* shows the proton-resonance absorption of a powdered specimen of potassium fluoride ($KF.2H_2O$).

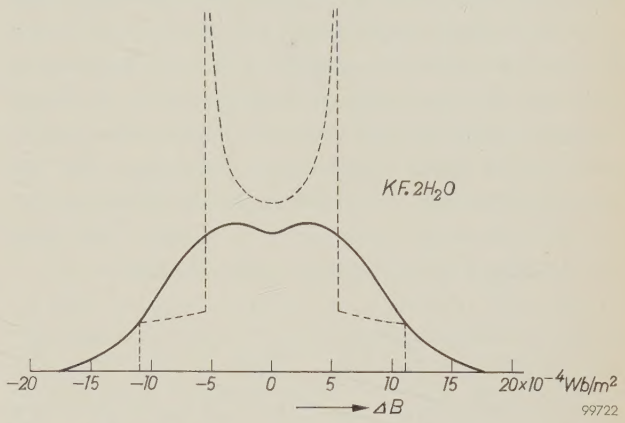

Fig. 2. Spectrum of the absorption caused by proton resonance in a powder sample of potassium fluoride ($KF.2H_2O$).
The dashed line represents the theoretical shape of the spectrum if there were only interaction between the protons of a single molecule of water. For calculating this curve the distance between the peaks was taken as 11×10^{-4} Wb/m^2, and the area below the curve was made equal to that under the experimental curve.

In the simple case of isolated proton pairs it is a fairly simple matter to predict a theoretical absorption curve that compares reasonably with the experimental result. In more complicated cases this is not so easy. In such cases, only the "second moment" of the broadened line is determined. If the line shape is given by

$$y = f(B),$$

its second moment is given by

$$\overline{(\Delta B)^2} = \int (B - B_0)^2 y \, dB \Big/ \int y \, dB.$$

If the value of $\overline{(\Delta B)^2}$ has been found experimentally, it can be compared with the theoretical value, for which Van Vleck derived the following [5]):

$$\overline{(\Delta B)^2} = C \sum_k \sum_{j \neq k} (3\cos^2\vartheta_{jk} - 1)^2 \, r_{jk}^{-6}.$$

Here r_{jk} represents the distance of a perturbing proton (j) to the perturbed proton (k), ϑ_{jk} the angle which the vector $\mathbf{r}$ makes with the external field, and C a constant comprising, among other things, the magnetic moments of the nuclei. The summation should really be extended over all the protons of the

[5]) J. H. van Vleck, Phys. Rev. **74**, 1168, 1948.

crystal, but in practice it is sufficient to take only a small volume element of about 10 Å diameter.

Let us now return for a moment to the magnitude of the broadening. Apart from the "static" mutual interaction of the ions, referred to above, there is also a dynamic interaction, resulting from the fact that the protons, owing to their precession about the direction of the field, generate local alternating fields as well as a local static field. It would be going too far to deal with the complete quantum-mechanical treatment of this problem, which takes into account both the static and the dynamic effects [6]). The result, however, is fairly simple, and states that the expression $(3\cos^2\vartheta - 1)$ occurring in the formula must be multiplied by a factor of $\frac{3}{2}$, making the total broadening $\frac{3}{2}$ times the static broadening.

If we consider only two protons, we see that they can orient themselves in three ways with respect to the field: both parallel, one parallel and the other anti-parallel, and both anti-parallel. This gives rise to three energy levels each being $\Delta E = 2\mu_z B$ apart (see formula 2).

The mutual interaction described above (analogous to two coupled pendulums) perturbs the energy levels. As a result, the separation of the energy levels is now:

$$\Delta E = 2\mu_z B_0 \pm 3\mu_z^2 r^{-3}(3\cos^2\vartheta - 1).$$

This means that resonance is found for

$$B = B_0 \pm \tfrac{3}{2}\mu_z r^{-3}(3\cos^2\vartheta - 1), \quad . \ . \ . \ . \quad (6)$$

which, except for the factor $\frac{3}{2}$, is the same as (5). The factor $\frac{3}{2}$ does not occur in the broadening caused by the influence of other nuclei on the protons, for which the static calculation gives the correct result.

Interaction with the crystal lattice

Apart from the interaction between the protons mutually and between the protons and other nuclei, interactions occur between the protons and the atoms of the specimen as a whole. This too gives rise to additional line broadening.

This additional broadening can be explained with the aid of Heisenberg's uncertainty principle. This tells us that the energy ΔE of an excited state is indeterminate by an amount δE, given by:

$$\delta E\, \delta t \approx h. \quad . \ . \ . \ . \ . \ . \ . \ . \quad (7)$$

The quantity δt in the present case is a "relaxation time" τ, the significance of which is as follows. In the absence of an external field the spin directions are randomly distributed owing to thermal equilibrium. If, at a given moment, all spins were made parallel, then as a result of interaction with the lattice this ordering would relax and ultimately vanish according to an exponential law:

$$e^{-t/\tau}.$$

In the case of protons in a liquid τ is of the order of 10 sec and therefore $\tau^{-1} = 0.1$ c/s. With the aid of (7) we find that this corresponds to an additional broadening of approximately 2×10^{-9} Wb/m^2. In solids τ may have a wide range of values, but the additional broadening here is almost invariably negligible compared with the other causes of line broadening.

Thus, although the interaction with the lattice or with the environment is often negligible as regards the effect on the line width, it is really essential to the occurrence of resonance absorption. In an external field B in which there are N protons, the number of parallel-aligned protons (N_1, state 1) at thermal equilibrium is greater than the number of anti-parallel-aligned protons (N_2, state 2), to an extent given by:

$$\frac{N_2}{N_1} = \exp(-\Delta E/kT), \quad . \ . \ . \ . \quad (8)$$

where T is the temperature and k is Boltzmann's constant ($k = 1.38\times10^{-23}$ J/°K). If, now, an alternating field of the desired frequency is applied, and if there were no interaction with the lattice, after some time a state would arise where $N_1 = N_2 = \frac{1}{2}N$. From that moment onwards as many protons would go over per unit time from state 1 to state 2 as from state 2 to state 1, and no absorption would be observed. The interaction with the lattice, however, tries to restore the situation (8); consequently, even when an alternating field is present, N_1 remains greater than N_2, and absorption can, therefore, still be observed. Also, it follows from this that, for the purpose of detecting the absorption, the alternating field should not be too strong. These points were already discussed in connection with paramagnetic resonance in the article quoted under [1]).

Structure of the spectrum in liquids

In contrast to crystals, where the line widths may cover 10^{-4} to 10^{-2} Wb/m^2, the resonance lines found for liquids are very narrow, of the order of, e.g., 10^{-7} Wb/m^2. Special measures, to be discussed later, are therefore necessary to keep the instrumental width (non-uniform field) below this limit. The fact that the marked line broadening found in crystals does not occur in liquids is due to Brownian motion which, in classical terms, so frequently perturbs the phase of the precessional movement that only the effect of the average field remains, the action of

[6]) See, for example, E. R. Andrew, Nuclear magnetic resonance, Cambridge Univ. Press, London 1955, pp. 152-154, 240-242.

neighbouring fields being eliminated by averaging with respect to time. The interaction with the medium remains as the sole cause of line broadening. As in crystals, however, this is a very slight effect.

The result of this situation is that, at field strengths of, say, 10^{-5} Wb/m^2, displacements and splittings of a resonance line are observed which are due to effects that may also be present in the solid but escape observation because of the large total broadening in the case of solids. These effects are largely attributable to the action of the magnetic fields of electrons. It is due to them that the spectra of various organic compounds differ so markedly from one another and can even be used for identifying these compounds. We shall deal with this subject at greater length when discussing the practical examples.

Equipment for nuclear-magnetic-resonance investigations

Investigations on liquids

As remarked, for observing nuclear magnetic absorption in liquids the magnetic field should be highly uniform. The field variation over the dimensions of the specimen (a few millimetres) should be less than $1 : 10^6$.

To obtain a sufficiently uniform magnetic field for these kinds of experiment, magnets are used, as mentioned above, in which the air gap is narrow compared to the diameter of the poles of the magnet. The pole pieces should be made of highly homogeneous material and ground optically flat. The remaining non-uniformity of the field is corrected by passing a current through suitably-positioned flat coils on the pole faces.

With the object of achieving a still higher resolution, the specimen is often rapidly rotated. This has a narrowing effect simular to that discussed above as regards the influence of the Brownian motion on the internal fields: the differences in macroscopic field strength are eliminated by averaging with respect to time. In this way a resolution of 10^{-8} Wb/m^2 can be achieved.

During the measurement the magnetic field should remain constant. In the case of an electromagnet, a highly stabilized current should be used, constant to within 10^{-6} of the desired value. Residual, relatively small fluctuations due to other sources are compensated by means of a coil of many turns wound round the magnet poles. The e.m.f. induced in this coil by a fluctuating magnetic field is amplified and converted into a current which is fed in anti-phase to a correction coil on the magnet. In this way a constancy of 3 in 10^8 can be maintained for several minutes.

An easier method to attain constant magnetic fields is to use a permanent magnet. The only important cause of deviations of the magnetic field in this case is that the magnetization of the magnetic material (e.g. "Ticonal") is temperature-dependent. The temperature of the magnet should change by no more than 10^{-4} °C if a constancy of 1 in 10^8 is to be attained. The magnet is therefore placed in a thermostat. Owing to the high thermal capacity of the magnet, a simple thermostat is sufficient to cope with the fluctuations of the ambient temperature.

The frequency of the applied alternating field, too, should have a stability of 1 in 10^8. This can be obtained by using a crystal-controlled oscillator placed in a thermostat. If a number of such crystals are available, various kinds of nuclei can be investigated. Since, however, as mentioned, nuclear magnetic resonance is mainly used for the investigation of organic compounds, the resonance of protons is of primary interest.

The variation of the magnetic field required for scanning the spectrum is produced by means of an additional excitation coil, through which a current is passed that rises very slowly and linearly from zero to a maximum (sawtooth waveform). In the case of a liquid spectrometer the maximum value of the field variation need only be quite small (a few 10^{-4} Wb/m^2).

Various types of high-resolution spectrometers are described in the literature, and some are also commercially available. As an example we shall mention some particulars of the high-resolution spectrometer marketed by Mullard (type SL 44 Mo2). This uses a permanent magnet which is accurately maintained at a constant temperature. The magnet gives a field of 0.9 Wb/m^2 and has poles of 15 cm diameter and a gap 3 cm in length. The resonance detector consists of a double-T measuring bridge, which is connected to a high-frequency amplifier, followed by a diode detector. The output voltage of this detector, which is proportional to the output voltage of the bridge, is applied to an oscilloscope having a long-persistence screen and to a recording unit. The bridge is fed by a crystal-controlled oscillator of 40 Mc/s. The specimen holder consists of a glass tube of 3 mm diameter, which is filled with the substance for investigation and rapidly rotated. The photograph in *fig. 3* gives an impression of the equipment. A block diagram appears in *fig. 4*; some additional details are given in the caption.

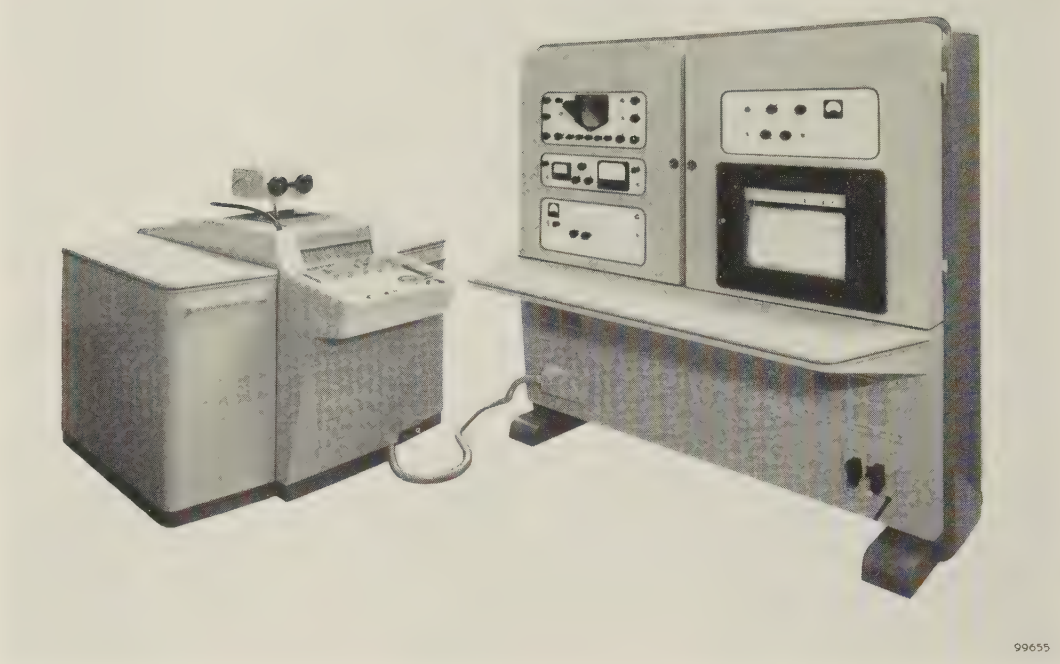

Fig. 3. Mullard equipment for nuclear-magnetic-resonance investigations on liquids (high-resolution spectrometer, type SL 44 Mo2).

Investigations on solids

Since the width of the lines in solids is generally very large (10^{-4} to 10^{-2} Wb/m^2), a highly uniform field is not necessary for absorption measurements on solids, nor need the field be so highly constant with time or the measuring frequency so stable.

On the other hand the absorption at a given field strength is now roughly a hundred times weaker. Compared with liquids, therefore, larger specimens are used and more sensitive equipment. The higher sensitivity is achieved by a different measuring procedure (see below). Higher demands are also made on the versatility of the spectrometer, since in solid-state investigations it may be necessary to measure the resonance of a large number of elements that may occur in crystals. Whilst the study of protons is often important for the determination of crystal structures (water of crystallization), the resonance of other nuclei (Cu, Al, etc.) enters into the study of *metals*. Investigation of the structure of the resonance line as a function of temperature, for example, makes possible the study of a number of effects (such as atom movements, which make the resonance line narrower, and diffusion phenomena).

As an example of a solid-state spectrometer we shall discuss the equipment used in the Philips Research Laboratories at Eindhoven. A block diagram of the set-up is shown in *fig. 5*.

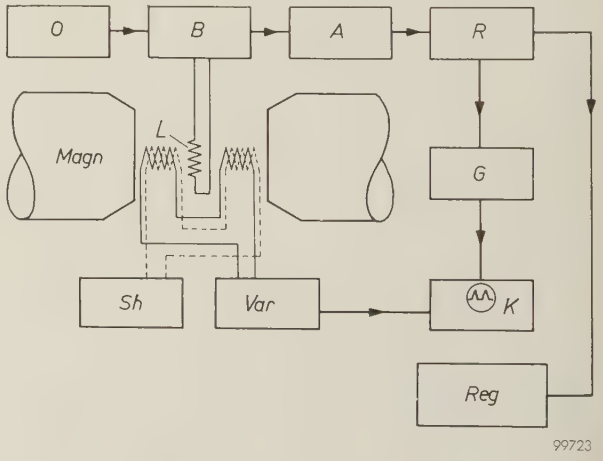

Fig. 4. Block diagram of the Mullard spectrometer in fig. 3 used for liquid analysis. *Magn* permanent magnet (induction in air gap 0.9 Wb/m^2). *L* alternating-field coil in which the sample is placed. *O* crystal oscillator, frequency 40 Mc/s, for generating the high-frequency alternating magnetic field inside the coil *L*. *B* measuring bridge. *A* preamplifier. *R* receiver. *G* diode detector. *K* cathode-ray oscilloscope. *Reg* recorder. *Var* generator of auxiliary current for the sawtooth variation of the static magnetic field used for scanning the spectrum. The current source *Sh* is used for correcting the magnetic field in the air gap to match it to the oscillating frequency of the crystal.

The field for this spectrometer is again generated by a permanent magnet. The fairly considerable range of field strengths required for the analysis of solids is obtained here by means of gaps of variable length in the yoke. With the aid of a cam the yoke bars can be raised, thereby decreasing the magnetic field. A particular advantage of this construction is that, within a certain range, the field can be reproducibly adjusted to any desired value, so that no auxiliary field is needed for matching to the oscillator frequency (cf. *Sh* in fig. 4).

The cam is driven by a synchronous motor via a gearbox, enabling the spectrum to be continuously scanned. The shape of the cams is such as to ensure the most linear possible variation of the field with time. As in the case of a high-resolution spectrometer, this is desirable in order that equal distances on the uniformly moving strip chart in the recorder will correspond to equal variations of B.

To the slow field variation a low-frequency sinusoidal modulation of very small amplitude is added (coils L_{mod} and oscillator O_{mod} in fig. 5). *Fig. 6* shows what happens. A portion of the resonance line of width δB is scanned. The resultant signal, when δB is sufficiently small, is proportional to the derivative dy/dB of the absorption curve $y = f(B)$.

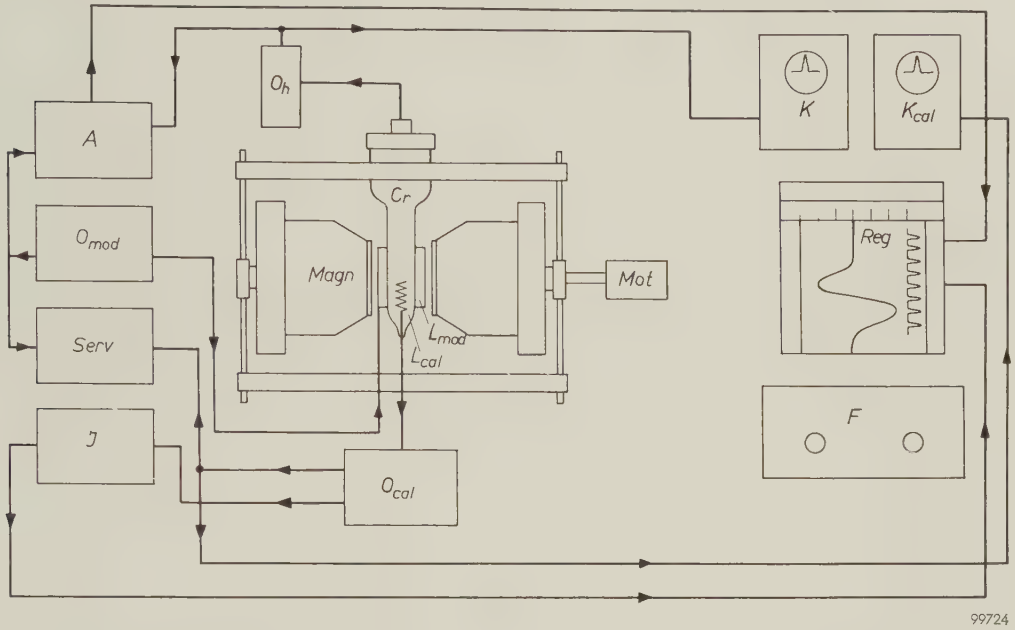

Fig. 5. Simplified block diagram of the solid-state spectrometer in Eindhoven. *Magn* permanent magnet (induction in air gap 0.45 Wb/m²). *Mot* synchronous motor with gearbox for shifting the yoke bars of the magnet, thereby effecting a continuous change of the field in the air gap (spectrum scanning). *Cr* cryostat, containing alternating-field coil and sample. O_h oscillator for generating the high-frequency alternating magnetic field in this coil. L_{mod} coils for the low-frequency modulation of the static magnetic field, fed by the oscillator O_{mod} (230 c/s). *A* selective amplifier. *K* cathode-ray oscilloscope for observing the output signal of O_h. *Reg* recorder. L_{cal} calibrating coil, used in conjunction with oscillator O_{cal} for calibrating the magnetic field by means of proton resonance. *Serv* servo amplifier, which keeps the calibrating oscillator tuned to proton resonance; this can be checked on the oscilloscope K_{cal}. *J* crystal-controlled oscillator with mixer stage, supplying the calibration pulses to the recording apparatus. *F* frequency meter.

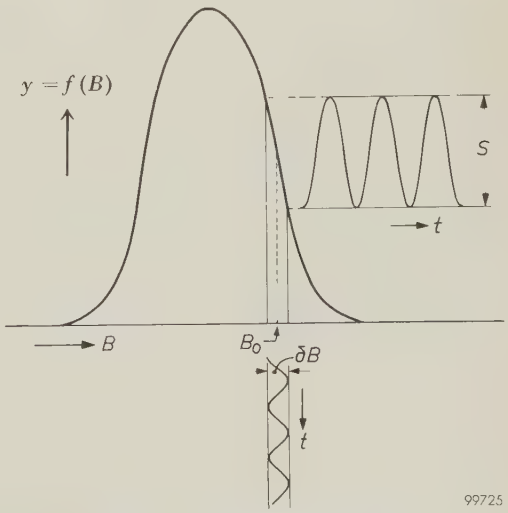

Fig. 6. Illustrating the scanning of a broad line by a low-frequency alternating magnetic field. The result, the derivative dy/dB of the absorption $y = f(B)$, is recorded. δB = modulation width, S = resultant signal.

This method of measurement has the advantage over the simpler method used for liquids that amplification is now possible in a very narrow band around the modulation frequency (230 c/s). As a result the unavoidable noise from the amplifier is suppressed and a considerable gain is achieved in the signal-to-noise ratio.

This method cannot be used with the liquid spectrometer because the line width, expressed in terms of frequency, is so very small (0.1 c/s). Modulation with a practical frequency, which must be at least thirty or forty c/s, would give rise to undesirable line broadening and satellite lines. However, since the absorption intensity in liquids is so much greater, a lower sensitivity is sufficient in their case.

The signal is detected, in the present equipment, with the aid of the same oscillator [7]) that supplies the high-frequency voltage to the alternating-field coil. This is done by making the coil form part of the frequency-determining network of the oscillator. A small change in the properties of the coil (the Q changes depending on the absorption of the specimen inside it) causes a considerable change in the voltage of the oscillator.

After detection the low-frequency signal is amplified in a narrow-band amplifier (A in fig. 5) and mixed with an alternating voltage whose frequency is equal to the modulation frequency. This finally produces a D.C. voltage which is proportional to the derivative of the resonance peak and is recorded on a strip chart. Examples of such recordings appear in fig. 10.

A second specimen and coil are present in the magnetic field. By means of proton resonance in this (liquid) specimen the magnetic field is continuously measured and calibrated by comparison with the signal from a crystal-controlled oscillator (J in fig. 5). The calibration marks appear on the recording. In the present equipment the distance between the marks is 1.17×10^{-4} Wb/m^2. This again clearly demonstrates the difference between the spectra of liquids and solids. Broadly speaking, about 20 calibration marks appear on one spectral line in the case of solids, whereas there may be 20 complete liquid spectra between two such calibration marks.

For measurements at low temperatures the complete specimen holder can be placed in a cryostat. With the set-up now in use, measurements can be made at temperatures as low as 20 °K; the recent availability of liquid He now makes it possible to measure down to 1.2 °K.

[7]) H. A. Thomas, Electronics **25**, January 1952, p. 114.

The caption to fig. 5 gives further particulars of the equipment. The photograph in *fig. 7* gives an impression of the set-up. The permanent magnet is shown separately in *fig. 8*, showing the mechanism for varying the air gap.

In the adjoining table some properties of the two nuclear magnetic spectrometers discussed are set out side by side.

	High-resolution spectrometer	Solid-state spectrometer
Specimen size	10 mm^3	1000 mm^3
Non-uniformity of the magnetic field over the whole of the specimen	$1:10^6$	$1:5\times10^4$
Instability of the static magnetic field with time	$1:10^8$	$1:10^5$
Instability of the alternating field	$1:10^8$	$1:10^5$
Resolving power $\Delta B/B$	$1:2\times10^7$	$1:5\times10^4$
Suitable for the nuclei:	especially ^{1}H, ^{19}F, ^{31}P	numerous
Modulation of static magnetic field	sawtooth	sawtooth + low-freq. sine wave
Amplitude of sawtooth	0.0002 Wb/m^2	0.03 Wb/m^2
Recorded quantities	absorption $y = f(B)$	dy/dB
Measurement at low temperatures	no	yes

There now follow some simple examples of the practical application of nuclear magnetic resonance.

Examples

The spectrum of ethyl alcohol

The ethyl-alcohol spectrum reproduced in *fig. 9* was recorded with a Mullard spectrometer. The spectrum consists of a number of very fine lines, and its total width is only 5×10^{-6} Wb/m^2. Since it is the spectrum of a liquid, the marked broadening usually found in solid spectra is lacking. The lines are due to hydrogen nuclei in the sample.

Let us now examine the structure of the spectrum more closely. There are three groups of lines. The integrated areas of each of the three groups are found to be in the ratio 3 : 2 : 1, corresponding to the formula CH_3-CH_2-OH. Why have these three groups a slightly different frequency and why is each group split into components (viz. 3, 4 and 1)?

The magnetic field at the position of one of the protons of the molecule is composed of the externally applied field plus the field produced by the surround-

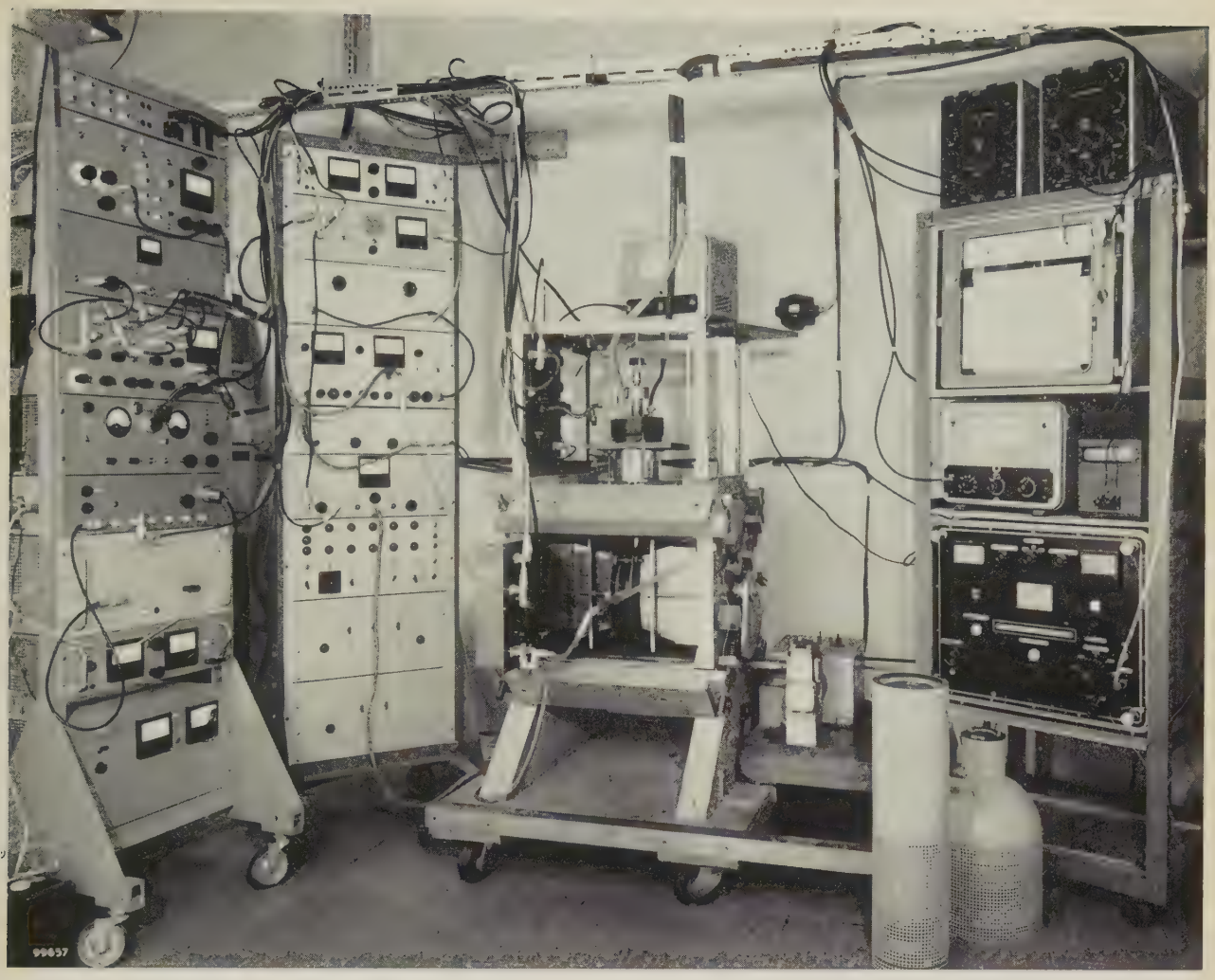

Fig. 7. Apparatus for the study of nuclear magnetic resonance in solids, in use at the Philips Research Laboratories, Eindhoven.

ing *valency electrons*. The electron density in the molecule is lowest in the OH group and highest in the CH_3 group, and for this reason the electron field differs for the three groups that make up the molecule. This causes the splitting into three groups of lines.

The splitting into components of a single group of lines arises as follows. The electrons move through the entire molecule and, as it were, communicate information to the nuclei regarding their immediate environment. Since, for example, the protons of the CH_2 group can assume different orientations in relation to the external field, the electron orbits can be polarized in different ways by the spin field of these protons. This gives rise to a change, albeit a very small one, in the magnetic field which the electrons produce at the position of the neighbouring groups. The two protons of the CH_2 group may either be both parallel with the measuring field, or one may be parallel and the other anti-parallel, or both anti-parallel. The total magnetic moment of

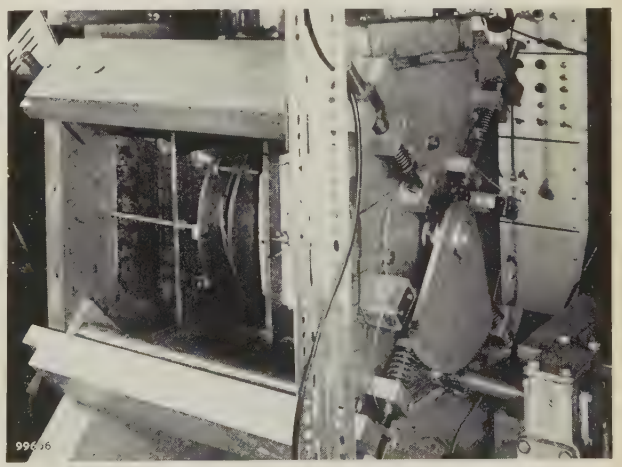

Fig. 8. The permanent magnet in the solid-state spectrometer at Eindhoven. On the right-hand side can be seen the toothed segment which is slowly turned by the motor via a gearbox (extreme right); attached to the segment is a cam which pushes the four radially mounted pins outwards. These raise slightly the four yoke bars, two of which can be seen in the photograph, thereby lengthening the total air gap in the magnetic circuit. This produces the desired time-linear variation of the magnetic field in which the sample is situated.

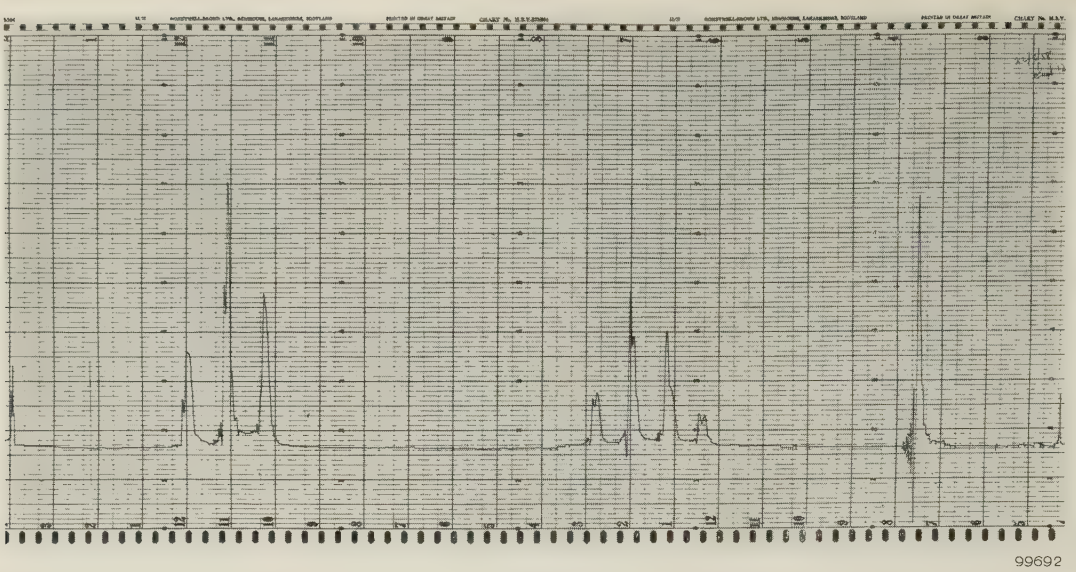

99692

Fig. 9. Spectrum of ethyl alcohol (CH_3-CH_2-OH), recorded with the Mullard spectrometer (fig. 3). In the spectrometer used, the magnetic field was 0.75 Wb/m^2.

the CH_2 group is then respectively $2\mu_z$, zero or $-2\mu_z$. The probabilities of these three cases occurring are in the ratio of 1 : 2 : 1. This causes the line belonging to the protons of the CH_3 group to be split into three components with an intensity ratio of 1 : 2 : 1. In the same way we can argue that the line pertaining to the protons of the CH_2 group is split, under the influence of the neighbouring CH_3, into four components with an intensity ratio of 1 : 3 : 3 : 1.

Special considerations apply to the line due to the OH group. One might expect that this line, under the influence of the neighbouring CH_2 group, would also be split into three components of intensity ratio 1 : 2 : 1. Only one line, however, is in fact found. The explanation is that the alcohol sample used contains *impurities* in the form of traces of water, acid or base. Since the electron density around the OH group is small, the proton of the OH group can easily break away. Where traces of impurity are present there is therefore a constant exchange between the H ion of the OH group and the H ions of the impurity. This proton exchange occurs for every molecule very many times per second. The time during which a proton of the OH group is under the influence of the polarized electron orbits in the alcohol molecule is therefore extremely short, and the average frequency of the exchange is high compared with the frequency difference between the splitting components of the line group, which would exist if there were no such exchange (approx. 10 c/s). As a result there is no effective splitting into components. In extremely pure alcohol the line of the OH group does show the expected splitting into three components.

The further details visible in the spectrum are due to second-order effects which do not enter into the scope of this simple explanation and will not be discussed.

It should be noted that the described spin-spin interaction, via the polarization of the electron orbits, differs essentially from the direct spin-spin interaction which occurs in solids and which, in our case, is made ineffective by the Brownian motion of the molecules.

The above inferences drawn from the nuclear magnetic resonance spectrum are an elegant confirmation of the structure of the alcohol molecule, already determined by other means. It is evident that in other cases valuable information can be obtained from liquid spectra, that can serve for determining an unknown structure.

The other examples to be discussed refer to solids. They concern investigations made, or still in progress, in Philips Research Laboratories at Eindhoven, and in all cases involve proton resonance.

Hardening of "Araldite"

The hardening of "Araldite" (Ciba, Basle) is a striking example of the transition of a fluid into the solid state. Araldite is a widely used synthetic adhesive of the epoxy-resin type. The adhesive consists of two fluid components, the epoxy resin and a hardening agent added and mixed just before use. After about 30 hours the adhesive has set hard as a result of polymerization of the epoxy molecules. Some spectra, recorded at various times during the hardening process, are shown in *figs. 10a, b* and *c*. It can be seen how the original very narrow liquid

line, whose width is determined by instrumental causes, develops into a solid-state line having a width of about 2×10^{-3} Wb/m^2. The variation of the second moment with time indicates that the line broadening takes place in several more or less distinct stages. This allows inferences to be drawn regarding the gradual slowing-down of the motions of various groups of atoms in the molecule. This subject has been studied more extensively by Lösche [8]).

Motion of hydrogen gas in metals [9])

The following example refers to the motion of hydrogen gas in metals. Some metals and alloys can absorb relatively large amounts of gas, e.g. hydrogen, and for this reason they can be used as getters in radio valves. One of these alloys is thorium-aluminium, Th_2Al. The crystal structure of this alloy has been extensively studied [10]), and it is found that a maximum of four atoms of hydrogen is taken up per molecule of Th_2Al. Between the metal atoms are two interstices, each of which can entrap two H atoms. We shall consider the compound Th_2AlH_2, in which half the number of available interstices are filled.

At room temperature a very narrow resonance line was found with this compound. Partly from the intensity distribution in the line it was concluded that this narrow line is due to protons that jump very rapidly from one interstice to a neighbouring unoccupied one. Owing to this movement the dipole-dipole interaction between neighbouring protons is averaged out. At low temperatures ($T < 100$ °K) a line width of 8×10^{-4} Wb/m^2 was found. Since 8×10^{-4} Wb/m^2 corresponds to a frequency difference of about 4×10^4 c/s, it may be inferred from this that under these circumstances the time spent by a proton in an interstice is long in relation to 3×10^{-5} sec. Measurement of the line width as a function of T produced the curve shown in *fig. 11*. From the temperature at which the line-narrowing begins, in conjunction with the value of the line width at low temperature, it is easy to determine the way in which the average jump frequency ν_s

[8]) A. Lösche, Arch. Sciences **10**, fasc. spéc., p. 197, 1957.
[9]) D. J. Kroon, C. van de Stolpe and J. H. N. van Vucht, Arch. Sciences **12**, fasc. spéc., p. 156, 1959.
[10]) P. B. Braun and J. H. N. van Vucht, Acta cryst. **8**, 246, 1955.

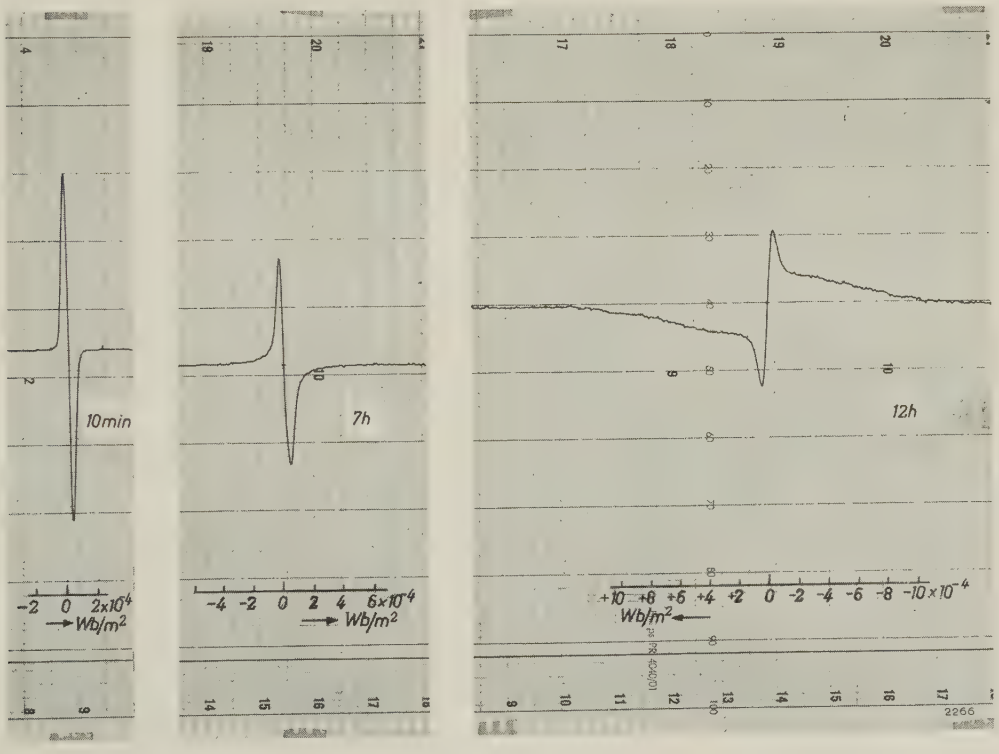

a *b* *c*

Fig. 10. Recordings of the derivative of the absorption of "Araldite" during hardening. *a*) Ten minutes after mixing. The width of the line is determined by the modulation width δB. *b*) Seven hours after mixing. The foot of the curve already shows some broadening. *c*) Twelve hours after mixing. The curve shows marked broadening.
The recordings were made with arbitrarily decreasing or increasing magnetic field; in (*a*) and (*b*) the field happened to be increasing, in (*c*) decreasing.

depends on the temperature. With a minor simplification this can be described by the formula:

$$\nu_s \propto \exp(-E_a/kT),$$

where E_a represents the activation energy of the diffusion process. This is found to be equal to 0.22 eV. From the intensity distribution of the absorption line it can be inferred that at low temperature short-range ordering of the protons exists. This investigation is being pursued.

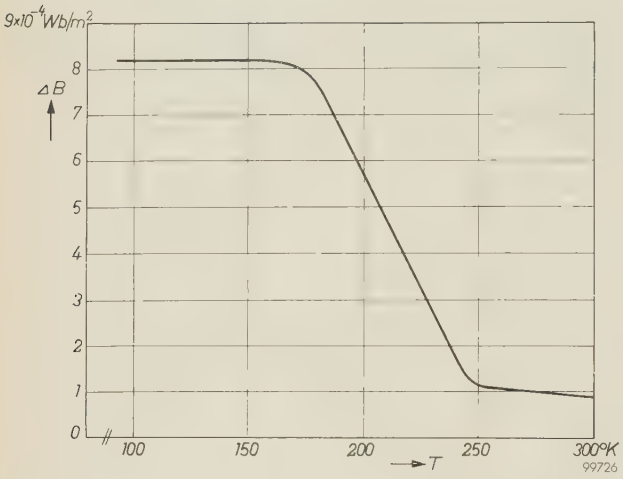

Fig. 11. Line width of the resonance in Th_2AlH_2 as a function of temperature.

Positions of protons in aluminium hydroxides [11])

To illustrate the application of the second-moment determination discussed above, we shall consider an investigation of aluminium hydroxide. Various hydroxides of Al are known, each with its own crystal structure; examples are hydrargillite (γ-$Al(OH)_3$), bayerite (α-$Al(OH)_3$) and boehmite (γ-AlOOH). We shall deal here with the first compound mentioned. The O atoms in this compound form a triangular layer structure. There are several conceivable sites for the H atoms; two are represented in *fig. 12a* and *b*. The theoretical value of the second moment (with an O-H distance of 0.96 Å) is 26×10^{-8} $(Wb/m^2)^2$ in the case *a*, and 29.4×10^{-8} $(Wb/m^2)^2$ in the case *b*. The value found by experiment is $(26.5 \pm 1.2)\times10^{-8}$ $(Wb/m^2)^2$, which argues in favour of the first assumption. Other crystal models that have been proposed give a widely different value, e.g. 15×10^{-8} $(Wb/m^2)^2$, and must therefore be rejected.

Finally, it may be noted that the few, very simplified examples of applications discussed here are by no means representative of all the possibilities offered by nuclear magnetic resonance. A list of the publications that have appeared so far on the subject of nuclear magnetic resonance would take up just as many pages as this article.

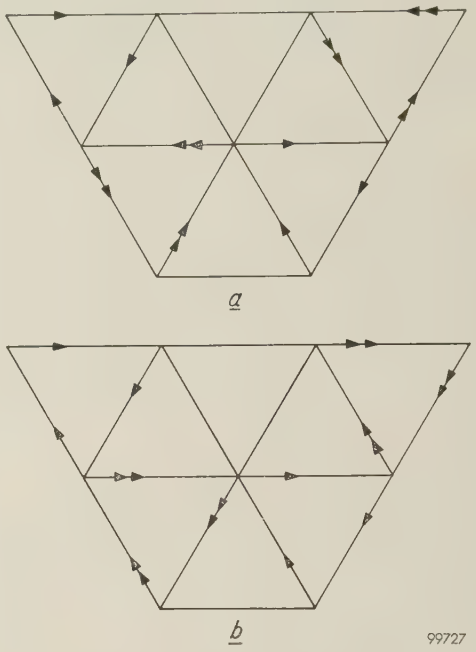

Fig. 12. In a crystal of γ-$Al(OH)_3$ layers of Al atoms alternate with double layers of O atoms. In the figure the O atoms are located at the corners of the triangles: in each case there are two O atoms one above the other at a distance apart of 2.79 Å. The H atoms are found between the two O layers; there are several theoretical possibilities as regards their precise position. (*a*) and (*b*) represent two possible configurations. In both cases each H atom lies on the oblique line connecting an O atom in one layer to a neighbouring O atom in the other layer, at a distance of 0.96 Å from one of these O atoms (the O-H bond length). These O-H bonds are indicated by the tail-ends of the arrows: a single arrow represents a bond with an O atom in the lower layer, and a double arrow a bond with an O atom in the upper layer. The result of nuclear magnetic absorption analysis argues in favour of the configuration (*a*).

Appendix: Comparison of nuclear magnetic resonance and paramagnetic resonance

In the introduction to this article mention was made of the relation between the phenomena of nuclear magnetic resonance and paramagnetic resonance. It is perhaps useful to touch here on some of the essential points of difference, some of which have already appeared in the foregoing pages.

The measurement techniques used for studying the two effects differ primarily in the wavelengths employed: paramagnetic-resonance investigations are performed at centimetric wavelengths, and thus use klystrons, waveguides and so on. Nuclear magnetic resonance is studied at wavelengths of some tens of metres, which calls for ordinary radio valves and transmission lines. This frequency difference is directly connected with the fact that the magnetic moment of the electron, which is equal to $eh/4\pi m$ (Bohr magneton), is roughly 1000 times greater than that of the proton or other nuclei. Nuclear moments according to equation (1) are principally given by $eh/4\pi m_P$ (nuclear magneton). As a result the two possible states for an electron (with a spin parallel or anti-

[11]) D. J. Kroon and C. van de Stolpe, Nature **183**, 944, 4th April 1959.

parallel to the external magnetic field) show an energy difference ΔE roughly 1000 times greater than that for a proton (see eq. (2)). Accordingly the frequency f_k at which nuclear magnetic resonance occurs (see eq. (4)) is given by:

$$f_k = g \frac{e}{4 \pi m_p} B,$$

and the frequency of paramagnetic resonance f_e (see eq. (5) in article [1])) is given by:

$$f_e = g_e \frac{e}{4 \pi m} B.$$

Since, for practical reasons, the magnetic fields B for observing the absorption due to electron spins and due to nuclear spins are chosen at the same order of magnitude (0.1 to 1 Wb/m^2), and since the numerical factors g and g_e in both formulae do not differ appreciably ($g_e \approx 2$, and g lies between 0.1 and 10, as mentioned earlier), we see that the resonance frequencies in the two methods differ by a factor of the order of 1000 (proton mass $m_p = 1836$ times electron mass m).

Another practical and very important difference between the two methods discussed concerns the sensitivity. The measurement of paramagnetic resonance is very much more sensitive than the measurement of nuclear magnetic resonance. This is again a direct consequence of the fact that for an electron the two possible states with opposite spin orientations show an energy difference ΔE about 1000 times greater than for a proton (confining ourselves now to protons). The relationship can be understood as follows. The difference between the numbers of protons and electrons in the two states mentioned is proportional to ΔE (see eq. (8), which is also valid for electrons). The number of electron spins that can contribute to energy absorption from the alternating field is therefore about 1000 times greater than the number of proton spins, the total number per unit volume being the same. Moreover the energy quantum ΔE absorbed from the alternating field upon each transition between the two states is also about 1000 times greater (this has already appeared in the frequency difference), so that the energy absorption — or the measured signal — other conditions being the same, is about 10^6 times greater for electrons than for protons.

True, the detectors used for centimetric waves give a much poorer signal-to-noise ratio than those for wavelengths of some tens of metres, and also the line width (to which the recorded intensity is inversely proportional) is several times larger in parametric resonance than in nuclear magnetic resonance. Nevertheless the first method referred to remains far more sensitive than the other, which means that paramagnetic-resonance investigations can be applied for very much smaller concentrations of resonators.

It is precisely for this reason that such useful results have been achieved with paramagnetic resonance: the paramagnetic centres are usually present in only low concentrations, whereas in nuclear-magnetic-resonance studies the whole of the investigated substance enters into the measurement.

This brings us to the last point of difference to be noted, which concerns the information obtainable with the two methods. Paramagnetic resonance provides information about the immediate environment of a paramagnetic centre. Nuclear magnetic resonance, on the other hand, gives information on the structure of molecules or of crystals as a whole, and on the effects of impurities (also non-paramagnetic impurities) on that structure.

A recent further development of the techniques discussed is the study of *double resonance*, where paramagnetic and nuclear magnetic resonance are excited in a substance simultaneously. This allows the nuclear magnetic resonance signal to be intensified, so that nuclei present in small concentrations are also accessible to investigation [12]). Moreover, the paramagnetic-resonance spectrum is influenced by the transitions between the energy levels of different nuclear spin orientations [13]). As a result still more particulars can be learned about the properties of the solid state. There is no space here, however, to deal at greater length with these methods and their application.

---

[12]) A. W. Overhauser, Polarization of nuclei in metals, Phys. Rev. **91**, 476, 1953. See also H. G. Beljers, L. van der Kint and J. S. van Wieringen, Overhauser effect in a free radical, Phys. Rev. **95**, 1683, 1954.

[13]) This method is also referred to as "Endor" (electron nuclear double resonance). See e.g. G. Feher, Electron spin resonance experiments on donors in silicon, Phys. Rev. **114**, 1219-1244, 1959 (No. 5).

Summary. Nuclear magnetic resonance gives rise to the specific absorption of electromagnetic waves (best measurable at metre wavelengths) by certain atomic nuclei, particularly hydrogen nuclei, when these are placed in a constant magnetic field. Since the resonance of a given nucleus is affected by the fields of neighbouring nuclei and electrons, the nuclear magnetic absorption spectrum offers a variety of information on the substance containing the nuclei. In solids the effect appears in a marked broadening of the resonance line; in liquids it appears in a splitting of the line into several components grouped closely together. A concise explanation of the theory of the phenomenon is followed by a description of two equipments used for recording the absorption spectra, one for liquids and the other for solids. The essentially different requirements of these two cases are dealt with at some length. In conclusion some examples are discussed of the numerous uses to which nuclear magnetic resonance has already been put, which include the identification of compounds (analysis of organic liquids) and the structural analysis of molecules and crystals

TEMPERATURES IN FITTINGS FOR INCANDESCENT LAMPS

by L. J. H. EXALTO.

536.4:628.95:683.865

For some years now there has been welcome evidence of increased activity in the design of lighting fittings, not only for the newer types of light source such as fluorescent lamps, but also for a source of long standing, the incandescent lamp. Presumably this activity has been stimulated by the post-war boom in housebuilding, by the evolution of public taste, and by the heightened interest of interior decorators in lighting matters. Decorators and others are experimenting with a variety of types of fitting, sometimes placing more emphasis on the aesthetic than on the functional aspect. Here it is for the public to decide whether they are prepared to sacrifice efficiency to appearance; but in any case safety must not be allowed to suffer. One aspect of the safety requirements relevant to incandescent-lamp fittings is dealt with in the article below.

Fittings for incandescent lamps must satisfy various safety requirements. In the first place the user must be safeguarded against accidently touching live parts. In the second place certain limits have to be imposed on the temperatures that arise under operating conditions. Obviously, a fitting that becomes excessively hot on the outside may represent a direct danger. If certain points inside the fitting become very hot there may be indirect danger too, in that conductors may short-circuit (an example is the point where the leads of the cord are splayed — point *s* in *fig. 1*) or come into contact with metal parts of the fitting and so make them live.

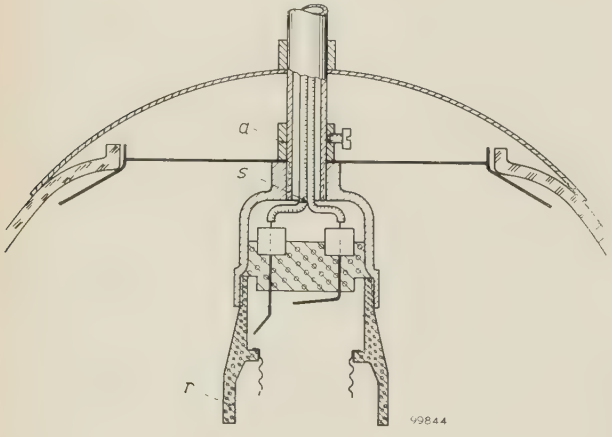

Fig. 1. Edison-type lampholder in fitting. The investigations involved the measurement of temperature of the lampholder rim (*r*), of the insulation of the cord at the point where the two conductors are splayed (*s*), of the ring containing the set-screw (*a*), and of various other points.

Details of safety requirements, and of test methods involving measurement of the temperatures arising in lamp fittings, are now being studied by the C.E.E. [1]). Fittings must, of course, be tested under conditions corresponding to heaviest loading in normal operation. This might mean inserting a lamp or lamps having the maximum wattage the fitting has been designed for. The matter is not as simple as all that, however, for the temperatures arising in a given fitting are not determined by lamp wattage alone, or in other words by the overall rate of heat production. They are dependent also on the temperature distribution within the lamp itself, which may be very different for different lamp types, as also upon the way in which heat is transferred to the fitting, i.e. upon the particular combination of conduction, convection and radiation operative therein: this last is dependent on the design and the shape of both lamp and fitting. All this makes it desirable that a standard heat source (called a "heat test source" by the C.E.E.) should be introduced for the purpose of testing fittings in a way that will allow their merits to be judged impartially.

The standard heat test source (to which we shall again refer at the end of this article) will have to be such that its heating effect is a reasonable approximation to that of a normal lamp. This aspect of the standard heat source has made it necessary to ascertain how various types of lamp behave in regard to the transfer of heat to the fitting. We shall now give some of the results yielded by extensive investigations undertaken by Philips in order to provide an answer to this question.

The first series of measurements we want to discuss relates to the simplest possible kind of "fitting" — a bare lamp suspended freely in still air from two copper wires. Of special interest here is the rise of temperature of the cap of the lamp above ambient. The rise in cap temperature may be attributed exclusively to conduction and to convection in the gas filling the bulb, processes which are influenced by the design of the filament and the dimensions of the lamp; radiation scarcely plays any part.

[1]) International Commission on Rules for the Approval of Electrical Equipment.

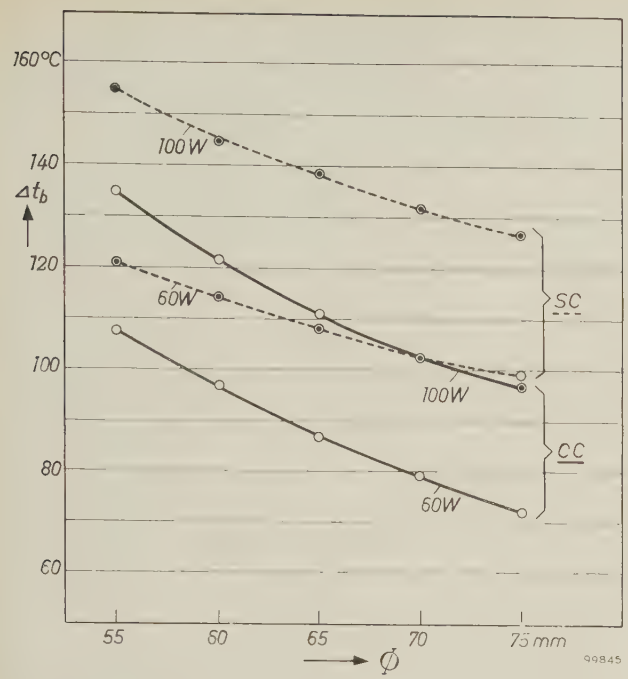

Fig. 2. The rise above ambient temperature of the rim of the cap of lighted incandescent lamps freely suspended from two copper wires in still air. This temperature rise Δt_b is plotted here as a function of Φ, the diameter of the glass bulb. The fully-drawn curves refer to 60 W and 100 W, 220-230 V lamps with coiled-coil filaments (CC). The broken curves refer to similar lamps with single-coil filaments (SC).

Some of the results of these measurements are displayed in *fig. 2*. The temperature rise of the rim of the cap, Δt_b, was measured [2]) in a series of gas-filled 220-230 V lamps of 60 W and 100 W ratings, some of which had single-coil and some coiled-coil filaments (indicated in the graph by the abbreviations SC and CC, respectively). Other things being equal, the amount of heat transferred to the gas filling is less in coiled-coil lamps than in single-coil ones [3]), and the former type could therefore be expected to produce lower values of Δt_b. To allow the influence of bulb size to be investigated, test lamps were made with diameters ranging from 55 mm to 75 mm in 5 mm steps, the other dimensions being adapted to the diameter (see *fig. 3*).

Fig. 2 shows that Δt_b increases as the lamp dimensions decrease. It also shows that, owing to the lower rate at which heat is transferred from filament to gas filling in a coiled-coil lamp, this type of lamp can be made with a bulb two or three steps of 5 mm smaller than that of a single-coil lamp of the same wattage, while retaining the same Δt_b value as the latter.

[2]) The method employed was that described in J. N. Bowtell, A method of measuring cap temperatures of general purpose tungsten filament lamps in free air, Light and Lighting **51**, 402-403, 1958.

[3]) This is precisely the reason why coiling the coiled filament results in higher luminous efficiency. See W. Geiss, Philips tech. Rev. **1**, 97, 1936 and **6**, 334, 1941.

Values of Δt_b considerably lower than those displayed in fig. 2 are found for vacuum lamps of the same wattage, likewise freely suspended in air. This is understandable, since there is no conductive or convective dissipation of heat via a gas filling; such dissipation in the gas-filled lamp has to be accepted in exchange for the higher filament temperature that is the favourable feature of the gas-filled as compared with the vacuum lamp (see for example the articles cited in footnote [3])). This point has been raised here in order to put the matter under discussion into true perspective: there is no case for abandoning the gas-filled lamp, with its far greater efficiency, just for the sake of reduced temperatures in fittings.

Having dealt with the bare lamp freely suspended in air, we shall go on to give results of temperature measurements on a fitting that may be regarded as an approximation to the other extreme. This would be a body closely enveloping the lamp and absorbing all the heat it gave off, including radiant heat. The temperatures of the various parts of a "fitting" of this kind would be entirely governed by the wattage of the lamp and, of course, by the provisions for cooling. The fitting actually investigated was made of metal, had a more or less conical shape, and was open at the bottom; no ventilation was provided for at the top of the fitting. The quantities measured [4]) included $\Delta t_s'$, the temperature rise at the cord splay point, and $\Delta t_d'$, the temperature rise in the metal

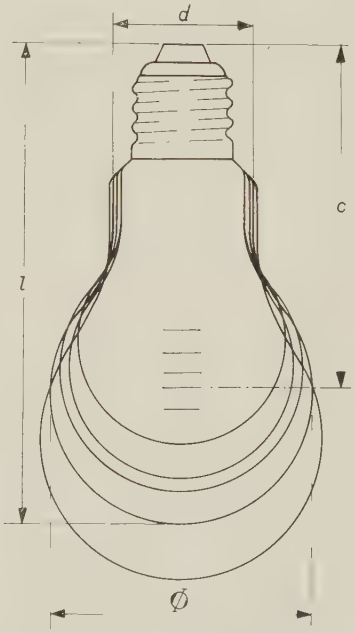

Φ	l	d	c
55	106	33	76
60	115	33	82
65	118	35	87
70	127	37	91
75	142	39	97

Fig. 3. Diagram showing dimensions of a series of incandescent lamps made for the purpose of the investigations. The lamps of the series had diameters Φ increasing in steps of 5 mm, the other dimensions being adapted to the diameter. The dimensions are given in mm in the table on the right. The horizontal lines lying roughly in the middle of the bulbs mark the position of the filaments. All the lamps had Edison-type E27/30 caps.

[4]) For a description of the method of measurement see H. F. Stephenson, The measurement of temperature in lighting equipment, Light and Lighting **47**, 369-372, 1954. (The same method is used by the C.E.E.) See also Flameproof electric lighting fittings, British Standard 889: 1947.

sleeve passing through the apex of the cone, the same series of lamps being investigated as in the case first discussed. In *fig. 4* these $\Delta t'$ values are plotted as a function of Δt_b, the temperature rise in the cap of the bare lamp, as given in fig. 2. It would seem that the conical fitting does not represent a very

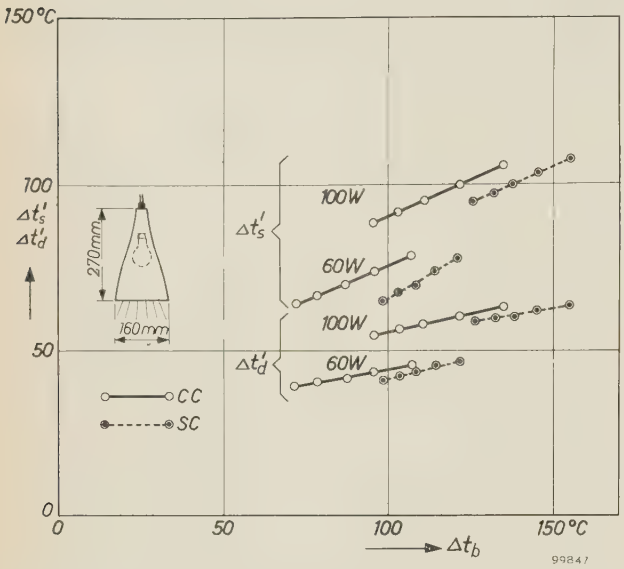

Fig. 4. Temperature rises measured with the same series of lamps as in fig. 2, inserted in a metal fitting of conical shape, open at the bottom and without ventilation at the top (see inset). The graph shows temperature rises $\Delta t_s'$ at the cord splay point, and $\Delta t_d'$ at the lead-in collar, as functions of Δt_b, the temperature rise undergone by the rim of the cap when the same lamp is freely suspended in air (fig. 2). As before, the fully-drawn curves relate to coiled-coil lamps and the broken curves to single-coil lamps. The five points through which each curve is drawn are the values measured (reading from left to right) for lamps with diameters of 75, 70, 65, 60 and 55 mm.

If the heating of the fitting were governed by lamp wattage alone, the curves would all be horizontal. If it were governed by Δt_b, the curves might be expected to pass approximately through the origin. The true state of affairs is evidently somewhere in between.

good approximation to the extreme case just alluded to (entirely enclosed fitting), since fig. 4 fails to demonstrate, except very roughly, that the temperature rises were determined only by the lamp wattage. Nor is another expectation borne out: it might be supposed that the temperature rise of the cap Δt_b would be representative of the heating effect of the lamp, i.e. that all $\Delta t'$ values for a given fitting would be mainly determined by Δt_b; it was to test this that we plotted our results in this particular way. If that supposition had been confirmed (and found valid for other forms of fitting), it would have been a comparatively simple matter to design standard heat sources for testing purposes. However, fig. 4 makes it quite clear that the facts are otherwise. Although there is unmistakably a correlation between Δt_b and $\Delta t_s'$ (say), it is a very incomplete one; for a given wattage the relative difference in $\Delta t_s'$ (or in the $\Delta t'$ value for some other point in the fitting) is very much less than the corresponding relative difference in Δt_b. This is clear from a comparison of lamps differing only in size, and it is even clearer from a comparison of lamps differing only in respect of filament design (CC and SC). Temperature rises in the fitting are thus but little affected by the considerable difference between the amount of heat dissipated via the gas filling in a CC lamp and that in a SC lamp.

Finally, *fig. 5* displays the results of similar measurements performed on an entirely enclosed fitting having the form of an opal-glass globe. A fitting of this kind may be regarded as an intermediate case between the two extremes already dealt with — the bare lamp and the metal cone. The points selected for temperature measurements were the cord splay point ($\Delta t_s'$) and the rim of the lampholder ($\Delta t_r'$). Qualitatively, and quantitatively too, up to a point, results for this fitting bear a resemblance to those obtained with the metal cone. The relative differences in $\Delta t_s'$ (and $\Delta t_r'$) appropriate to different lamps are again considerably smaller than the corresponding relative differences in Δt_b. It was also found, as before, that the lamp wattage was by no means the only factor determining $\Delta t'$ values. However, one wattage rule does apply to both forms of fitting: replacing a 60 W by a 100 W lamp of the same design (i.e. with the same kind of filament — SC or CC — and the same dimensions) leads to an approximately 40% increase in Δt values. Furthermore, the results for the two forms of fitting corroborate the important conclusion that can be drawn from fig. 2,

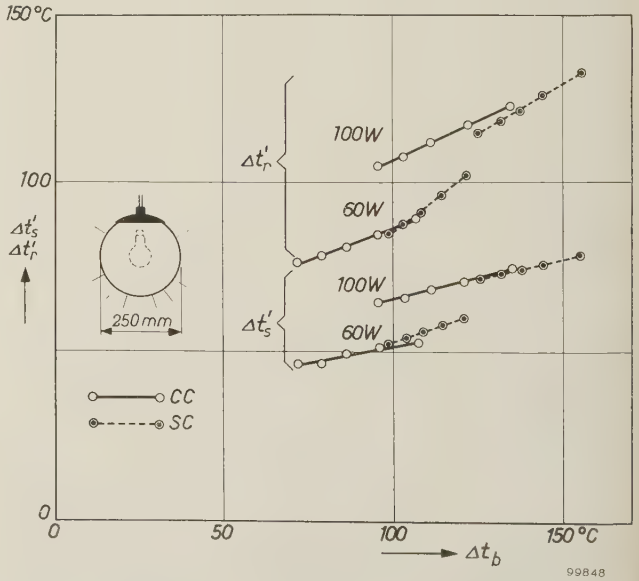

Fig. 5. Temperature rises measured inside an opal-glass globe (see inset) and plotted in the same way as in fig. 4. The temperature rises measured were $\Delta t_s'$, at the cord splay point, and $\Delta t_r'$, on the lampholder rim.

namely that, all other things being equal, smaller temperature rises are obtained with a coiled-coil filament than with a single-coil one. Hence, if the fitting has the form of a metal cone or an opal-glass globe, it is permissible (insofar at least as the points measured are concerned, which are, however, representative of the fitting as a whole) to use a CC lamp that is one or two steps of 5 mm smaller than a SC lamp.

The results given above — a very brief summary of extensive investigations, not yet concluded — provide no more than a rough guide in the approach to the problem of standard heat test sources. Even so, the results obtained so far are sufficiently revealing to justify a first attempt at making such sources. They will have to be provided with a normal lamp base, so that they can be inserted in fittings, and they will have to give off heat in much the same way as a normal incandescent lamp does; in other words, the sources will essentially be incandescent lamps (whose light yield, however, is of no interest). The experiments make it clear that it is not sufficient to specify certain Δt_b values: the wattage and mechanical design of the standard heat test sources, as well as their Δt_b values, will likewise have to be laid down in the specifications. A tentative specification for such heat sources is now in preparation. Practical tests will be necessary to assess their effectiveness.

Summary. For the testing of lighting fittings as regards their heating-up, it is desirable that standard heat test sources should be used in place of ordinary lamps. The problem is to design sources that will simulate, with reasonable exactness, the heating effect of incandescent lamps of the types that would normally be used in the fitting. Extensive investigations into this heating effect, carried out with lamps of different wattages and sizes in different fittings, have led to the conclusion that temperature rises are not governed entirely by the wattage or the Δt_b (temperature rise of cap of bare lamp freely suspended in air). Another important conclusion is that lamps with a coiled-coil filament cause smaller temperature rises in fittings than single-coil filament lamps that are otherwise completely similar.

A TRANSISTOR CARDIOTACHOMETER FOR CONTINUOUS MEASUREMENTS ON WORKING PERSONS

by G. A. HARTEN and A. K. KORONCAI.

53.083:612.16

Measurement of the heart rate is an important means of estimating the energy consumption of the human body and for ascertaining whether a person is subjected to needless physical strain when working under adverse conditions. The value assumed by the heart rate consists of a component related to the energy consumption of the body and of an extra component that may be due to a variety of factors, such as excessive ambient temperature, an awkward stance — certain muscles are then constantly contracted, which hinders the circulation in them — nervous tension, smoking and so on.

The relation between the first component and the energy consumption of the body can be determined in the laboratory in various ways with reasonable accuracy, and then correlated with the oxygen consumption, which is a direct measure of the energy consumed. Thus, if the heart rate and oxygen consumption are measured simultaneously, the magnitude of the extra component can be calculated [1]).

Omitting the oxygen-consumption measurement and determining only the heart rate does not, it is true, provide an exact indication of the energy consumption, but it still gives the physician a reasonable insight into the way in which the subject reacts to his work — unless the extra component is exceptionally large. Roughly speaking, rates of 70 to 80 beats per minute correspond to light (sedentary) work, 80-100 to moderately heavy work, and 100-130 to very heavy work. Of course, the terms light, heavy, etc., have no absolute significance here, but indicate how the subject himself (to judge from his heart rate) reacts to the work. When fatigue sets in, the extra component increases and so, therefore, does the heart rate.

The normal way of determining the heart rate by feeling the pulse is obviously not practical in an investigation of this kind; one cannot keep hold of a subject's pulse while he is working. If the subject suddenly stops what he is doing, the heart rate usually changes so quickly that a measurement taken immediately after the interruption already shows a quite considerable error, even when the pulse is taken for a period of only 10 seconds.

An apparatus has been developed at Eindhoven that makes it possible to measure the heart rate of working persons at any desired moment, and if necessary continuously, without obstructing their movements [2]). *Fig. 1* shows the equipment worn by the subject. The principle is as follows. Fixed to the subject's ear is a small clip, one side of which carries an electric bulb and the other a phototransistor type OCP 71. With each heart beat the blood stream

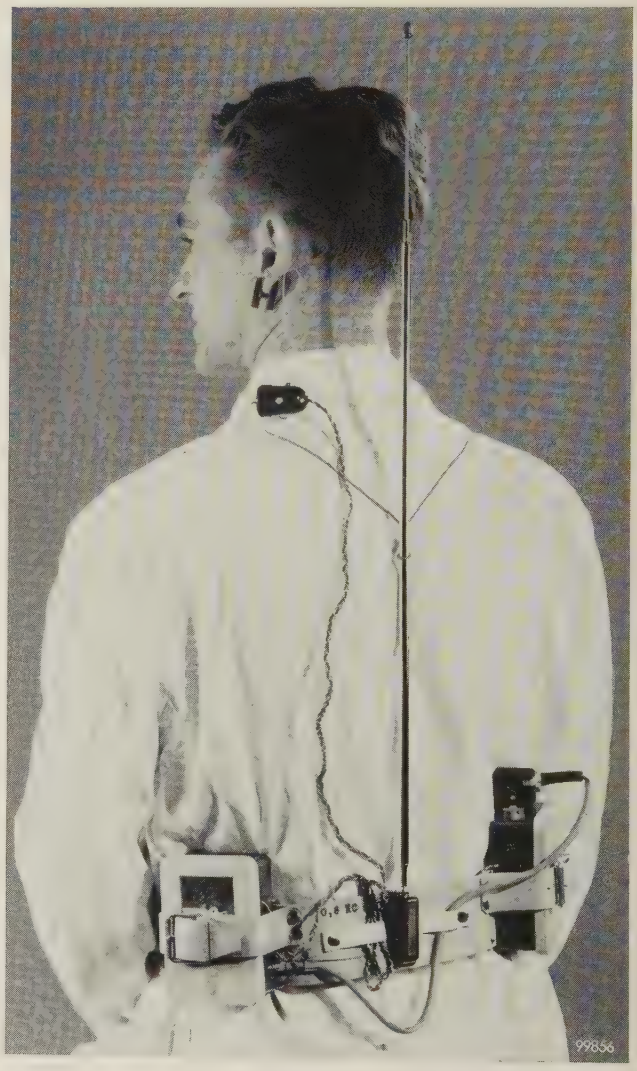

Fig. 1. The part of the apparatus worn by the subject. The subject is not obstructed in his movements.

[1]) See G. J. Fortuin, G. A. Harten, G. de Maar and P. A. van Wely, Tijdschr. soc. Geneesk. **37**, 389, 1959 (No. 10).

[2]) The same principle has been used by E. A. Müller and J. J. Reeh, Arbeitsphysiologie **14**, 137, 1950; E. A. Müller and W. Himmelmann, Int. Z. angew. Physiol. **16**, 400, 1957; and D. H. Bekkering and H. J. van Dal, Report No. 13, Research Inst. Public Health Eng., T.N.O., The Hague, June 1952. Literature referring to other equipment for cardiotachometry is quoted in the latter two papers and also in A. W. Melville and J. B. Cornwall, Electronic Engng. **31**, 268, 1959.

changes momentarily the amount of light transmitted through the ear lobe, and the current through the phototransistor therefore changes correspondingly. The resultant voltage pulses are conducted, after amplification, to a pulse shaper which delivers a square-wave signal upon every heart beat. This pulse signal triggers, via a transistor switch, a fixed-frequency oscillator (frequency about 3000 c/s) which amplitude-modulates the carrier frequency of a miniature transmitter (frequency 10 to 15 Mc/s). The signal from this transmitter can be picked up by a normal radio receiver.

Interference in the receiver due to other signal sources could be reduced if the carrier frequency of the transmitter were raised to about 100 Mc/s and frequency modulation adopted. An ordinary receiver could then still be used, but there would now be less interference from broadcast stations. Furthermore, the receiving aerial in this case could be directed towards the subject.

Each heart beat, then, is heard as a short high-pitched note, and the observer is able to count the number of beats occurring in a period of 10 or 15 seconds.

The pick-up element (*figs. 2* and *3*) and all other components mentioned, including the transmitter,

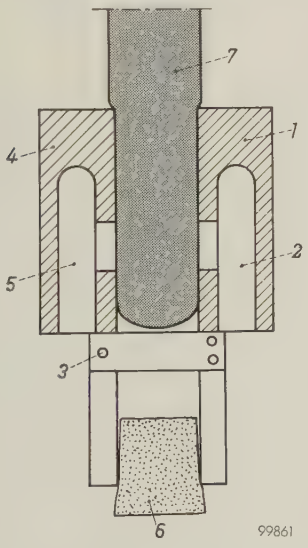

Fig. 2. Ear clip for electric bulb and phototransistor. *1* fixed arm with space *2* for bulb. *3* hinge pin. *4* hinged arm with space *5* for phototransistor. *6* foam plastic functioning as spring. *7* lobe of ear.

are very small and light and do not hamper the subject in his work. The way the apparatus is worn has been seen in fig. 1. Altogether the equipment weighs about three pounds. Except for the phototransistor, the entire electronic circuit (see *fig. 4*) is contained in the case on the right. The other case

Fig. 3. Showing how the clip is attached to the ear and how the wires are arranged so that they will not cause undue interference by communicating their movements to the clip. The clip itself weighs about $2\frac{1}{2}$ grams; the spring tension should not exceed 20 to 30 grams.

contains 18 small nickel-cadmium storage batteries and a potentiometer for adjusting the current through the electric bulb. The aerial is a normal telescopic type as used on cars. The apparatus can work for 8 hours before the batteries need to be recharged. This takes 10 to 12 hours.

To reduce interference, the amplifier is designed to pass only frequencies in a band of about 1 to 3 c/s, i.e. 60 to 180 heart beats per minute (see *fig. 5*). The chief causes of interference are the mains (hum) and unduly sharp movements of the subject. Interference signals of the latter kind have a frequency of the order of 10 c/s. If there is a powerful source of infra-red radiation near the subject, the ear must be screened; infra-red and also visible red radiation are passed fairly well by the ear, and the phototransistor reacts to radiation up to wavelengths of about 1.5 μ [3]).

If frequent or continuous measurements are called for, simple counting of the audible pulses by an observer is evidently inconvenient. We have therefore designed a recording count-rate meter for the

[3]) See e.g. F. H. R. Almer and P. G. van Zanten, An experimental pyrometer using a phototransistor and designed for radio-tube inspection, Philips tech. Rev. **20**, 89-93, 1958/59 (No. 4).

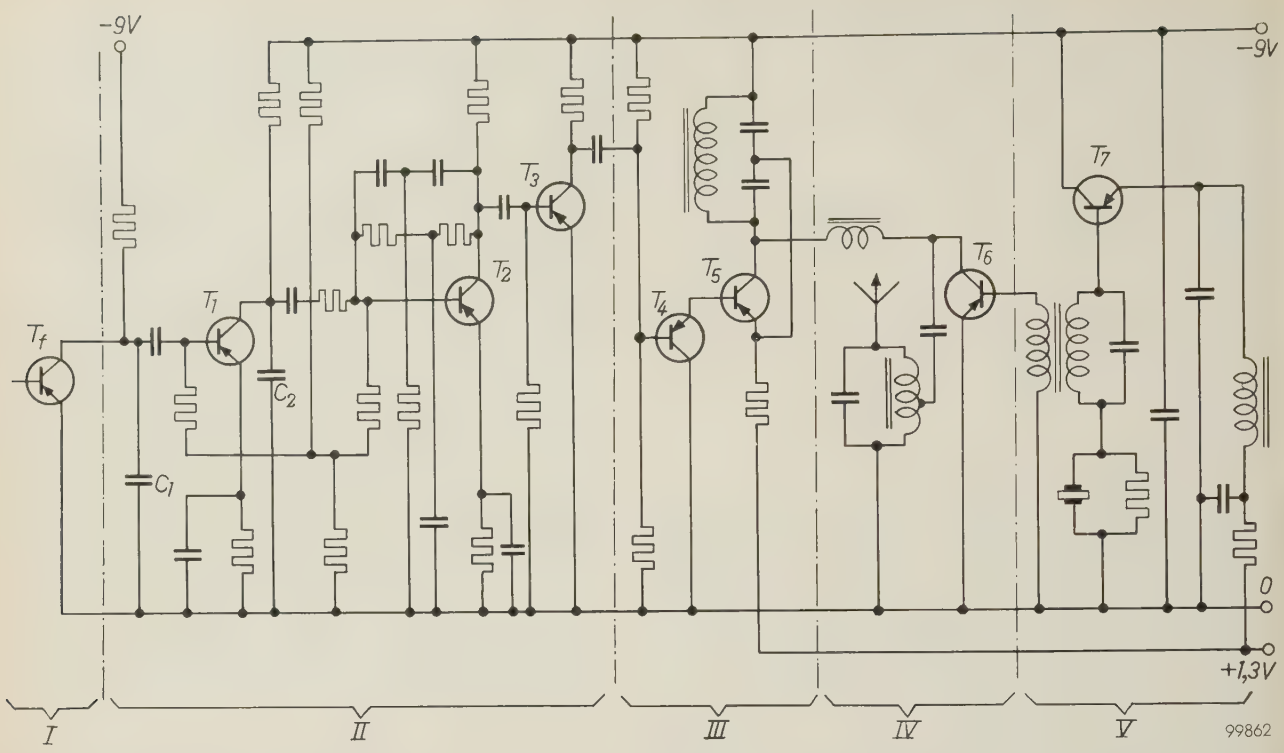

Fig. 4. Electronic circuit of apparatus carried by subject. On the left, in section *I*, is the phototransistor T_f, which is mounted in the ear clip. Section *II* contains the selective amplifier and pulse shaper. The required frequency response is obtained by means of a double T-filter [4]) and capacitors C_1 and C_2 (1.6 μF). Section *III* contains a 3000 c/s oscillator (transistor T_5), triggered into oscillation by a switching transistor T_4 while the shaper circuit in *II* delivers a pulse. This oscillator modulates the carrier frequency (10-15 Mc/s) of the transmitter. The latter consists of a crystal-controlled transistor oscillator (section *V*) inductively coupled to an output stage (section *IV*). The phototransistor T_f is fed from a separate voltage source. The circuit in section *II* is encapsulated in a plastic block measuring 35×35×70 mm. Sections *III* and *IV* are together in a similar block measuring 30×35×90 mm, and section *V* in another block of the same size.

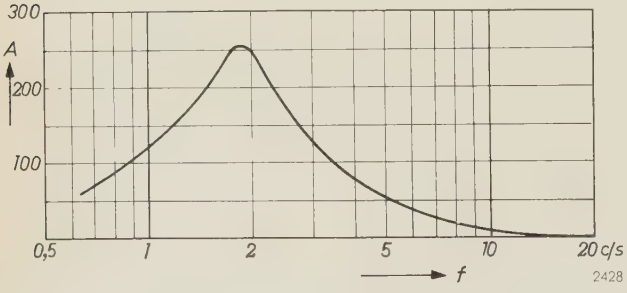

Fig. 5. Frequency response (voltage gain *A* versus frequency *f*) of amplifier (section *II* in fig. 4). At frequencies outside the range from 1 to 3 c/s the gain is less than half the maximum.

purpose. A block diagram of the instrument is given in *fig. 6*. Block *1* is the radio receiver, which gives a short-lived signal of 3000 c/s at every heart beat. This signal passes to block *2*, in which it is fed to a selective amplifier that only passes frequencies in a narrow band at 3000 c/s (to limit interference), and is then converted into a rectangular pulse. Block *3* contains a count-rate circuit consisting of a monostable flip-flop followed by a diode pump circuit [5]) and an *RC* network in which a meter *4* is incorporated. The time constant of the *RC* network is approximately 5 seconds. The meter indication is thus in a sense an average of the heart rates that occurred in the 5 to 10 seconds prior to the moment

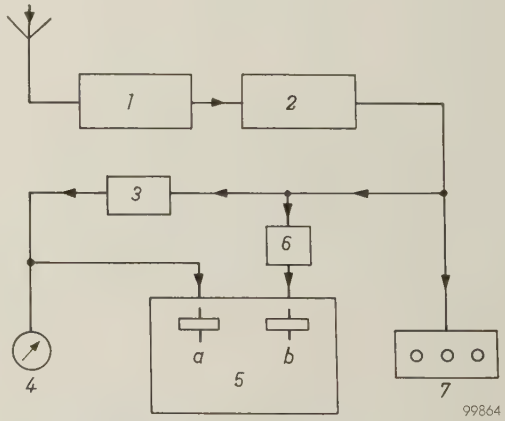

Fig. 6. Simplified block diagram of apparatus for measuring and recording the heart rate. *1* radio receiver. *2* selective amplifier (3000 c/s) with pulse shaper. *3* count-rate circuit. *4* meter with scale from 1 to 3 c/s (60 to 180 beats per minute). *5* recorder; the stylus *a*, like the meter *4*, receives the output signal from the count-rate circuit. *6* circuit enabling the stylus *b* of *5* to record *rapid* variations of the heart rate. *7* electrical counter.

[4]) The properties of these filters are described in D. H. Smith, Electronic Engng. **29**, 71, 1957.

[5]) The diode pump circuit is dealt with extensively in J. B. Earnshaw, Electronic Engng. **28**, 26, 1956. A recent application is described in J. J. van Zolingen, Philips tech. Rev. **21**, 134-144, 1959/60 (No. 4/5), on page 138 *et seq.*

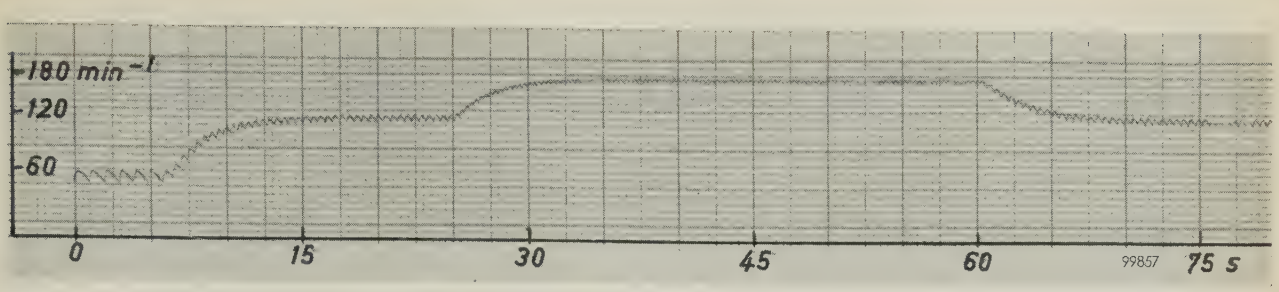

Fig. 7. Recording of the output signal from the count-rate circuit (block *3* in fig. 6) at frequencies of 1, 2 and 3 c/s (60, 120 and 180 beats per minute). The recording stylus drops back slightly between two beats. The response time here is about 12 seconds.

of taking the reading. Of course, the meter cannot follow very rapid changes of heart rate, but the response time is short enough for most cases encountered. If the *RC* time constant is made shorter, the needle deflection drops appreciably between successive heart beats, and consequently the indication is more difficult to read. The value mentioned proved to be a useful compromise between the readability of the meter and its response to the variations of the heart rate. The circuit is designed to allow the meter scale to cover a frequency range from 1 to 3 c/s. The output signal of block *3* can also be recorded by the stylus *a* of the recorder *5* (see *fig. 7*).

For following *rapid* variations of the heart rate, use can be made of the circuit *6* in fig. 6. This delivers sawtooth pulses whose amplitude is a measure of the time elapsing between two heart beats (*fig. 8a* and *b*). When these pulses are recorded and a line drawn through their peaks, the resulting curve is effectively that which would be obtained by a recording frequency-meter having a very short indication time [6]). The recorder itself will produce this curve directly if the paper is made to move slowly enough (fig. 8*c*). The paper speed should not, of course, be so reduced as to lose the advantage of rapid indication.

Block *7* in fig. 6 represents an electrical counter, equipped with cold-cathode tubes, that counts all pulses (heart beats) and can therefore be used when the observer wishes to make a direct count of heart beats over a given period.

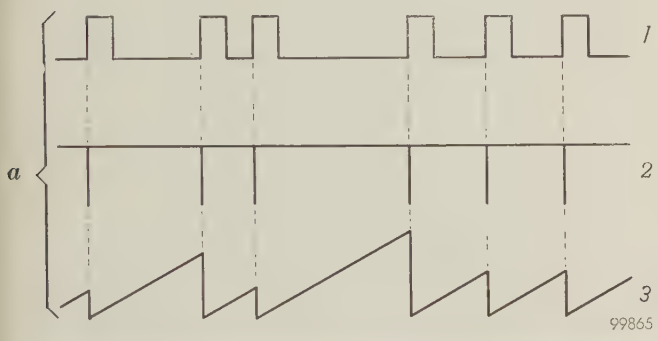

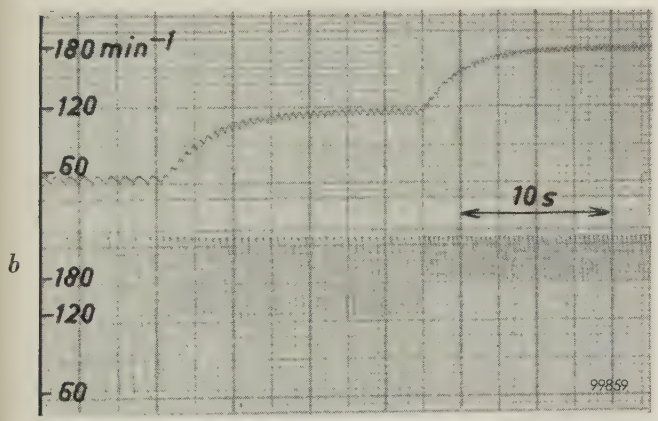

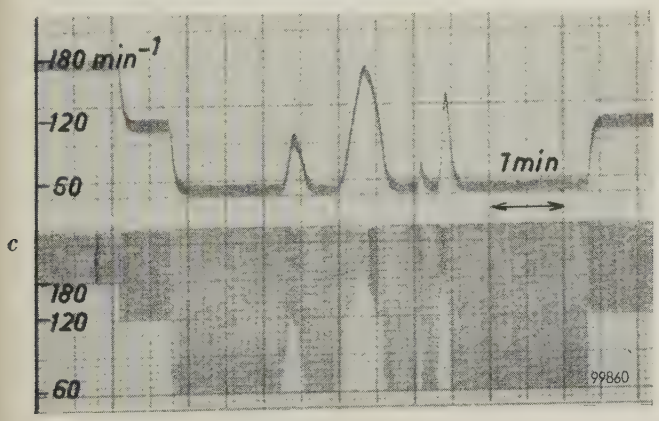

[6]) The idea of applying this method to the present case is due to G. Klein of this laboratory.

Fig. 8. *a*) The circuit in block *6*, fig. 6, operates in the following way. The output pulses *1* from block *2* (obtained by rectifying the 3000 c/s signals) are applied to a pulse shaper that converts them into pulses *2* of much shorter duration (about 3 ms). These pulses, via a transistor circuit, discharge a capacitor, which charges up again in the time between two pulses. The voltage across this capacitor shows the waveform *3*. The height of the sawtooth voltage peaks is a measure of the time interval between successive heart beats.
b) Above: recording of the output signal from the count-rate circuit. Below: recorded output signal of circuit mentioned under *a*). The applied frequencies were successively 1, 2 and 3 c/s in both cases. A line drawn through the peaks (the envelope) of the lower trace can be regarded as originating from a count-rate meter having a very short response time.
c) The same curves recorded in a practical case. By reducing the speed of the paper the envelope referred to is obtained automatically in the form of the demarcation line between the written and unwritten parts of the paper.

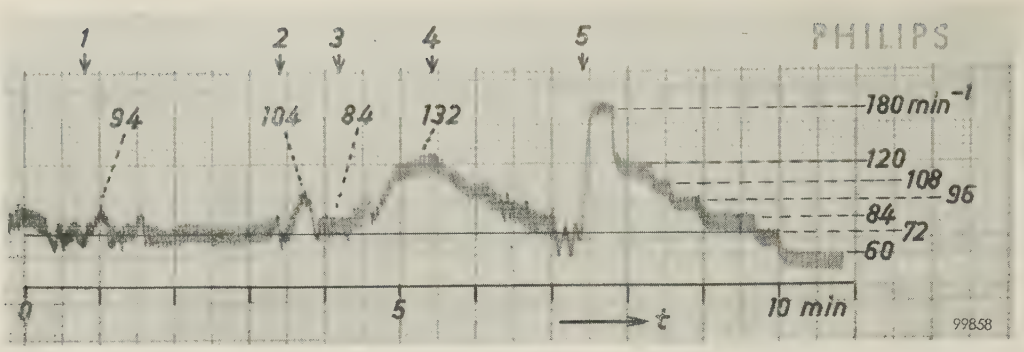

Fig. 9. Recording of heart rate versus time t (left, up to the point 5). Initially the subject is seated. At *1* he shifted his chair for a moment and then remained quietly seated. At *2* he stood up and remained standing; about 25 seconds after the action of standing up, the heart rate has returned to a virtually constant but somewhat higher value than when the subject was seated. Between *3* and *4* the subject performed twenty deep knees-bend exercises and then sat down again (at *4*). After 2 minutes the heart rate has returned to the normal value when seated. On the right, from *5* onwards, the recording was made from an "artificial heart" to obtain the calibration marks shown.

If the subject does not have to shift from one place to another during his work, and need make no considerable movements, wireless communication is evidently superfluous. The output signal from the pulse shaper that drives the 3000 c/s generator can then be applied directly to the measuring and recording instrument (fig. 6, blocks *3* to *7*). This does away with the interference produced by the radio receiver picking up signals of different origin. Moreover, the subject then carries no other equipment than the ear clip and leads. The other apparatus can be set down beside the count-rate meter and recorder.

An example of the way the heart rate reacts to various kinds of bodily movement is given by the recording in *fig. 9*. The calibration marks on the graph were obtained with the aid of an "artificial heart", consisting of a metronome to which a small plate is attached. With each swing of the metronome the plate interrupts the path of light between a lamp and a phototransistor. This device also supplied the pulses required for recording figs. 7 and 8.

Summary. Investigations into the physiological aspects of work call for a means of continuously measuring the heart rate of persons engaged on their normal work, where it is evidently not feasible to take the pulse in the normal way. In the apparatus described the individual heart beats are converted into electrical pulses by arranging for a beam of light transmitted through the lobe of the ear to fall on a phototransistor. Each pulse causes a miniature transistorized transmitter to transmit a note of 3000 c/s on a carrier of 10-15 Mc/s. Together with aerial and Ni-Cd batteries, this part of the equipment weighs about 3 lb and is carried on the back. The transmitted signals are picked up by a conventional radio receiver and either counted directly or applied to a recording count-rate meter (range 1-3 c/s; time constant $\sim$5 sec). Rapid changes in heart rate can be faithfully recorded by means of a special circuit that supplies pulses whose amplitude is a measure of the time between two heart beats.

AUTOMATIC CONTROL OF A FILAMENT-COILING MACHINE WITH THE AID OF PRESET COUNTERS

by F. EINRAMHOF and P. HAVAS. 621.326.652.3:621.778.3-52

In manufacturing certain types of filaments for incandescent lamps the filament-coiling machine is usually controlled by a cam mechanism. This method is not particularly convenient when it is desired from time to time to switch the production to different types of filament. This article describes an electronic control circuit incorporating cold-cathode tubes, in which the lengths of the coil sections can be adjusted by means of switches.

Special-purpose incandescent lamps, e.g. for studio lighting, film projection and coastal navigation lights normally have filaments composed of a number of coiled sections spaced by sections of uncoiled wire (*fig. 1*).

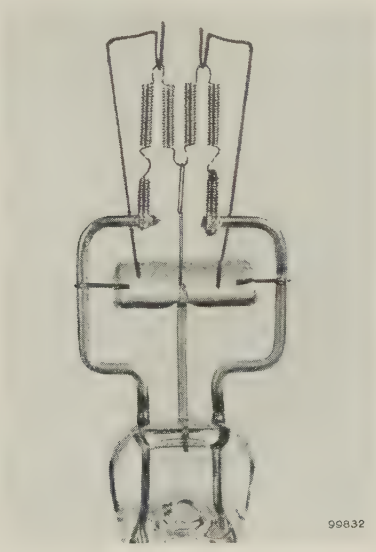

Fig. 1. Filament composed of four parallel coiled sections (See Th. J. J. A. Manders, Incandescent lamps for film projection, Philips tech. Rev. **8**, 72-81, 1946, page 74.)

There are two methods of manufacturing these filaments. In the first method the wire is coiled into a continuous helix. Afterwards the straight sections are made by straightening one turn at the appropriate location. If the straight sections have to be longer than the length of a single turn, the second method is adopted. Here the straight parts are produced automatically: the winding machine produces a coil interrupted by straight sections of wire.

For the second method the winding machine must be controlled according to a certain programme, which was hitherto realized mechanically by means of cams. For changing over to the manufacture of another type of filament, certain gears in the camshaft drive have to be exchanged. For large runs this can hardly be called a drawback, but for small runs a more flexible form of control is preferable. It is all the more desirable for development work on filaments for new applications or for improvements to existing types. One important problem is attaining the optimum temperature distribution within the filament. For systematically investigating this matter, the lengths of coil sections and gaps must be varied independently. With cam-motion control this would become a costly and elaborate operation.

An electronic device using preset decade counters, i.e. counters giving a voltage pulse when reaching a preset number, has now been designed for the control of filament-coiling machines. The preselected programme can be easily and rapidly changed by means of a few switches. An experimental set-up of a simple filament-coiling machine controlled by this circuit will be discussed here.

Description of the coiling machine

A sketch of the coiling machine is shown in *fig.* 2. A bobbin *S* with tungsten wire is fitted to winding

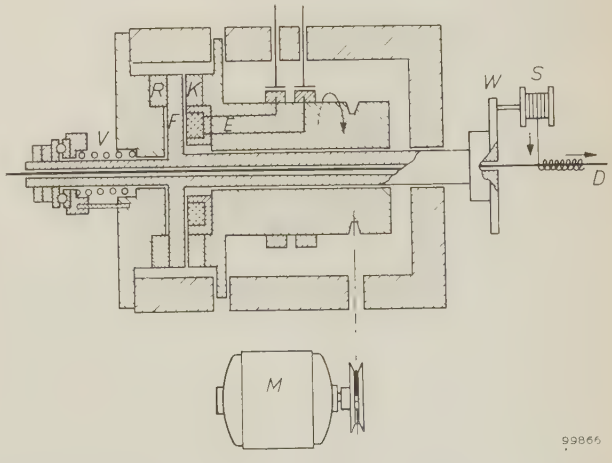

Fig. 2. Sketch of the winding machine. *M* motor. *W* winding head. *S* bobbin with tungsten wire to be wound on mandrel *D*. *F* flange fitted to the winding-head spindle. *E* electromagnet, which, when energized, pulls the flange against clutch plate *K*, so that the winding head is driven by the motor. *V* spring, pressing the flange to braking disc *R* when the electromagnet is not energized, thus stopping the winding head.

head W. When electromagnet E is energized, flange F is pulled to the right against clutch plate K; the winding head is now driven by the motor. When E is no longer energized, the disc is pressed by spring V to braking disc R and the winding head is stopped. The wire is coiled around a mandrel D moved axially through the winding-head spindle by the motor. (This mandrel is subsequently dissolved in acid, so that only the coil remains.)

Winding a filament composed of, e.g., three coiled sections and three straight parts is done in the following stages.

a) The motor is running and the electromagnet is energized, hence the mandrel is moving and the winding head is rotating, so that the first coiled section is being wound.

To stop winding, the current through the electromagnet must be interrupted. If this were to happen with the motor running at full speed, some slip would occur because the brake cannot immediately bring the head to a standstill. The pitch of the coil would therefore increase and the coil would be too long. Besides, the slip of the head is not always uniform, so that deviations from the nominal lengths cannot be prevented by interrupting the current at an earlier moment. The speed of the winding head must therefore be reduced first. This comprises the next stage, viz.:

b) The motor is switched off, whilst the electromagnet remains energized. The motor is running out but winding is still continuing at decreasing speed.

When the speed of the winding head has dropped sufficiently, the electromagnet is cut out, stopping the winding head. At the same time the engine is revved up again for the third stage.

c) The motor is running, but the electromagnet is not energized. The mandrel is now moving but no winding takes place, so that a straight section of the filament is being formed.

The coil is thus made in stages (*a*) and (*b*), the straight part in (*c*). For the next coil-and-straight section these three stages are repeated, so that a filament comprising three such sections is made in nine stages. The velocities of motor spindle and winding head during four successive stages are shown in *fig. 3*.

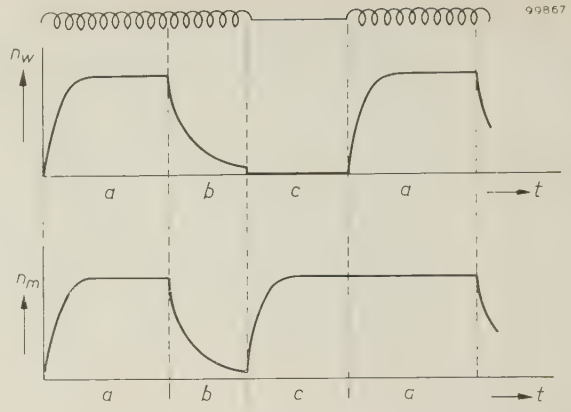

Fig. 3. Rotation speeds n_m of the motor spindle and n_w of the winding head as functions of time: *a* coil winding at full speed, *b* winding at decreasing speed, *c* formation of straight section of filament. The coil thus produced is shown schematically above the diagrams.

Principle of the control circuit

Each stage must be switched on as soon as the preceding stage is complete, i.e. as soon as the coil has the necessary number of turns or the straight section has the determined length. This implies, in each case, that the motor spindle has then completed a certain number of revolutions. If the entire process is to take place automatically, a device is required to count the number of revolutions of the motor spindle, and to produce a switching pulse when this number is reached. These numbers must be readily reset to make it possible to vary the lengths of the coils and straight parts independently of each other.

For counting the number of revolutions of the motor spindle the latter is fitted with a disc P with ten apertures (*fig. 4*). On one side of the disc is a lamp L, on the other side a phototransistor Tr which triggers a transistorized pulse generator I ten times per revolution. The pulses from I (height 80 V, length 25 μsec) are applied to a decade counter Te, consisting of four decade-stages of cold-cathode tubes. The maximum counting capacity is 9999 pulses, or a 1000-turn coil, with an accuracy of 1/10 turn.

The counter is connected to a programmer unit PB, likewise comprising cold-cathode tubes. When the preset number of pulses has been counted, the programmer applies a signal to switching unit SB upon which the latter energizes motor and/or electromagnet for the next stage. At the same time the counter is reset to zero, so that the number of pulses of the next stage can be counted.

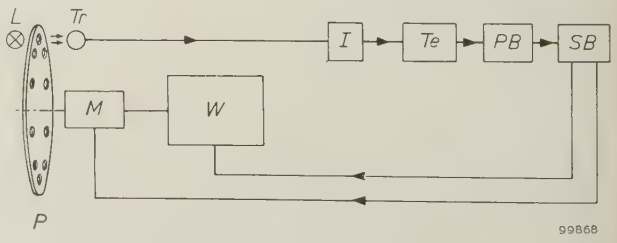

Fig. 4. Block diagram of the winding machine with electronic control. W winding machine. M motor. P perforated disc on motor spindle. L light source. Tr phototransistor. I pulse generator. Te counter. PB programmer unit. SB switching unit.

The counter circuit described here thus gives a switching command when the preset number is reached, unlike decade counter tubes such as the E 1 T [1]), which only *indicate* the number of pulses counted.

The counter

The cold-cathode gas-discharge tubes employed are of the type Z 70 U (*figs 5a* and *b*). Apart from cathode and anode, this tube contains two auxiliary electrodes, viz. a trigger electrode and priming electrode arranged as second cathode. This latter

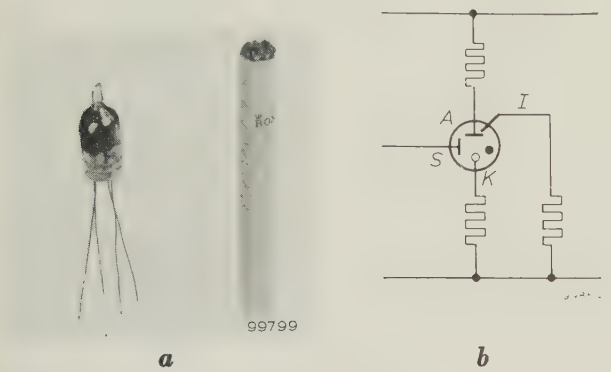

a *b*

Fig. 5. *a*) Cold-cathode gas-discharge tube, type Z 70 U. *b*) Schematic diagram. *A* anode. *K* cathode. *S* trigger electrode. *I* priming electrode. A small discharge current is permanently present between priming electrode and anode, to minimize the delay in establishing the main discharge.

electrode is fitted very close to the anode, so that a priming discharge is initiated by an extremely small current (3 μA); to limit the priming current to this small value the priming electrode is earthed via a high resistance. The priming discharge ensures that ions are always present within the tube, so that the main discharge is established more quickly. The trigger voltage (trigger-cathode) to initiate the main discharge is 145 V; the burning voltage between cathode and anode is 120 V.

Each decade stage comprises 10 tubes, circuited as shown in *fig. 6*. The +80 V pulses to be counted are applied to input *I*. Consider the situation when only valve *0* is conducting. This tube then has a cathode potential of 100 V; the trigger electrode of tube *1* has the same potential. When the next counting pulse reaches the input, the triggering voltage of tube *1* is exceeded, so that now this tube ignites. The pulse is likewise supplied to the triggers of the other tubes, but these do not ignite as they have as yet no trigger bias.

When tube *1* ignites, tube *0* extinguishes. The cathode of tube *1* initially remains at earth potential owing to the presence of C_{k1}, so that a large current flows through tube *1*. This current temporarily sets up a high voltage across the common anode resistor R_a, so that the anode voltage of all tubes drops. The cathode of tube *0*, however, is still maintained at 100 V by C_{k0}, so that the anode-cathode voltage of this tube drops below the burning voltage. Whilst tube *0* extinguishes, tube *1* remains conductive, because the cathode potential of the latter tube is as yet low, so that here the anode-cathode voltage does *not* fall below the burning voltage. While the voltage across C_{k1} rises towards 100 V, the current through tube *1* decreases.

Because tube *1* is now conducting, a 100 V bias is applied to the trigger of tube *2*, so that upon the next pulse the latter tube ignites and tube *1* extinguishes. Each successive tube is similarly ignited. The number of the tube conducting at any given moment thus indicates the total number of pulses received.

The maximum counting rate is determined by two factors. Once a tube has been ignited by a counting pulse, the next counting pulse must not arrive before the cathode voltage of this tube (and hence the bias of the next tube) has reached 100 V. It is accordingly the *RC*-time of the cathode circuit that determines the counting rate. This is moreover restricted by the time necessary for initiating the discharge. The present circuit has a maximum counting rate of 2000 pulses/sec.

When tube *9* is conducting, the next pulse has to initiate two events. First it has to ignite tube *0* of its own decade. This means that tube *0* must receive its bias from tube *9*. The ten counter tubes are accordingly arranged as a ring circuit. Secondly a pulse must be applied to the next decade. That is why the first decade is equipped with an additional tube, the "relay" tube *D* (fig. 6), arranged in a self-quenching circuit. *D* is biased when tube *9* is conducting, and will be fired by the next counting pulse. The relay tube, however, is not directly connected to the common anode resistor of the decade, but via a second resistor R_a' of sufficiently high value to prevent a sustained discharge within the tube. A capacitor C_a is connected in parallel with the anode resistors, allowing the tube to fire for a moment, but quenching it as soon as the voltage across this capacitor has been built up. This means that the cathode voltage just reaches 100 V for a moment and then drops to zero. The latter pulse is trans-

[1]) See the article: A. J. W. M. van Overbeek, J. L. H. Jonker and K. Rodenhuis, A decade counter tube for high counting rates, Philips tech. Rev. **14**, 313-326, 1952/53.

The preset decade counter employed and the programmer-tube circuits described below were developed by L. Wasser and E. Strauman of Philips AG Zurich.

A similar counting circuit for an entirely different application was described some years ago: J. Domburg and W. Six, A cold-cathode gas-discharge tube as a switching element in automatic telephony, Philips tech. Rev. **15**, 265-280, 1953/54.

mitted from the output *O* to the input of the next decade.

In this way the four decades are connected in cascade. The indication of the counter is given by the trigger tubes themselves which light up when ignited, behind windows with the appropriate numbers.

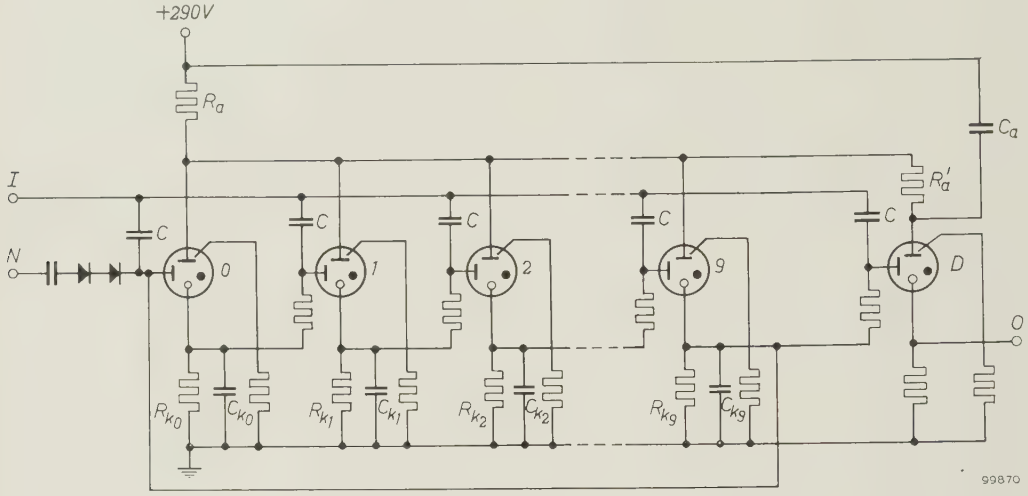

Fig. 6. Decade of a decade counting circuit employing cold-cathode tubes (Z 70 U). *0-9* counting tubes. *D* relay tube. *I* input. *C* input capacitors. R_a common anode resistor. R_a' additional anode resistor for tube *D*. C_a reservoir capacitor whereby *D* passes a short current pulse when fired. *O* output to the next decade. *N* input for the reset pulse, for returning the counter to zero.

For resetting the counter to zero, a +300 V pulse is applied (at *N*) to tube *0* of all four decades. This is sufficient to ignite these tubes even if they have no bias, whilst the temporary drop in anode voltage extinguishes all other tubes. Reset to zero is commanded by the programmer unit, which produces a 100 V voltage pulse for this purpose. This voltage is applied to the zero-reset tube, a cold-cathode tube supplied with a permanent bias from a voltage divider. Like the relay tube of a decade, it is arranged in a self-quenching circuit and therefore produces only a pulse of current. This current is stepped up to the required 300 V by a transformer.

The programmer unit

The programmer unit also incorporates cold-cathode tubes of type Z 70 U, viz. one tube per decade for each stage of the coiling process. The circuitry of such a programmer tube is shown in *fig. 7*. The tube gets its trigger bias from another programmer tube. The trigger of the tube is connected, via an input capacitor *C* and a 10-position switch, to the cathode of one of the counting tubes of a decade. When the decade reaches the preselected number on the switch (except zero, see below), a voltage of +100 V relative to earth is applied to *C*. The charging current of this capacitor causes a voltage pulse across resistor *R* that will fire the tube if the trigger electrode has the necessary bias.

The operation of the complete circuit of counter and programmer tubes may now be explained with the aid of the block diagram of *fig. 8*. Like the tubes of each counting decade, the programme tubes P_1-P_{36} are arranged in a ring. The tubes P_1-P_4 correspond to the number indicating the desired length of the first coiled section of the filament; let us assume that in the counter the number 6527 has

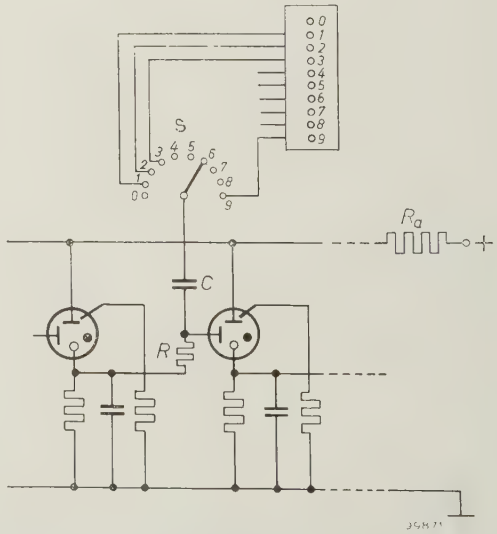

Fig. 7. Cold-cathode tube as programmer tube. The ten-position switch *S* connects the trigger electrode of the tube to the cathode of one of the counting tubes of the decade. The tube is biased via the cathode of the preceding programmer tube and then fires when the counter indicates the appropriate number. The programmer tubes have a common anode resistor R_a.

been preselected. This means that the trigger of P_1 is connected to the cathode of tube *6* of the thousands decade, P_2 to tube *5* of the hundreds decade, P_3 to tube *2* of the tens decade and P_4 to tube *7* of the units decade. Before the winding process is started, the counter is set to zero and the bias is applied to P_1. The motor is now started, so that count pulses are applied to the input of the counter. When the thousands decade changes to *6*, P_1 ignites. This produces the bias for P_2. Now the next occasion that the hundreds decade reaches *5*, P_2 can fire. 6500 pulses have now been counted. P_1 extinguishes again and P_3 is biased. Then, after 6520 pulses, P_3 will fire and similarly, after 6527 pulses, P_4.

The cathode of P_4 then has a voltage of 100 V. This is used to start the next stage as follows.

1) The voltage is transmitted to a switching unit, which changes the activation of motor and magnet as required for ending the first stage in the winding process and starting the second stage.
2) The voltage is applied to the zero reset. The counting decades are thus set to zero and are immediately ready for counting the second number of pulses.
3) P_5 is biased.

Whilst the second stage is being completed, valves P_5-P_8 are successively ignited, after which the third stage is started. In this way the entire programme is completed. The last tube of the ninth stage applies again the bias to P_1, so that production of the next filament starts without interruption.

In position *0* the ten-position switches have a function different from that described above. Con-

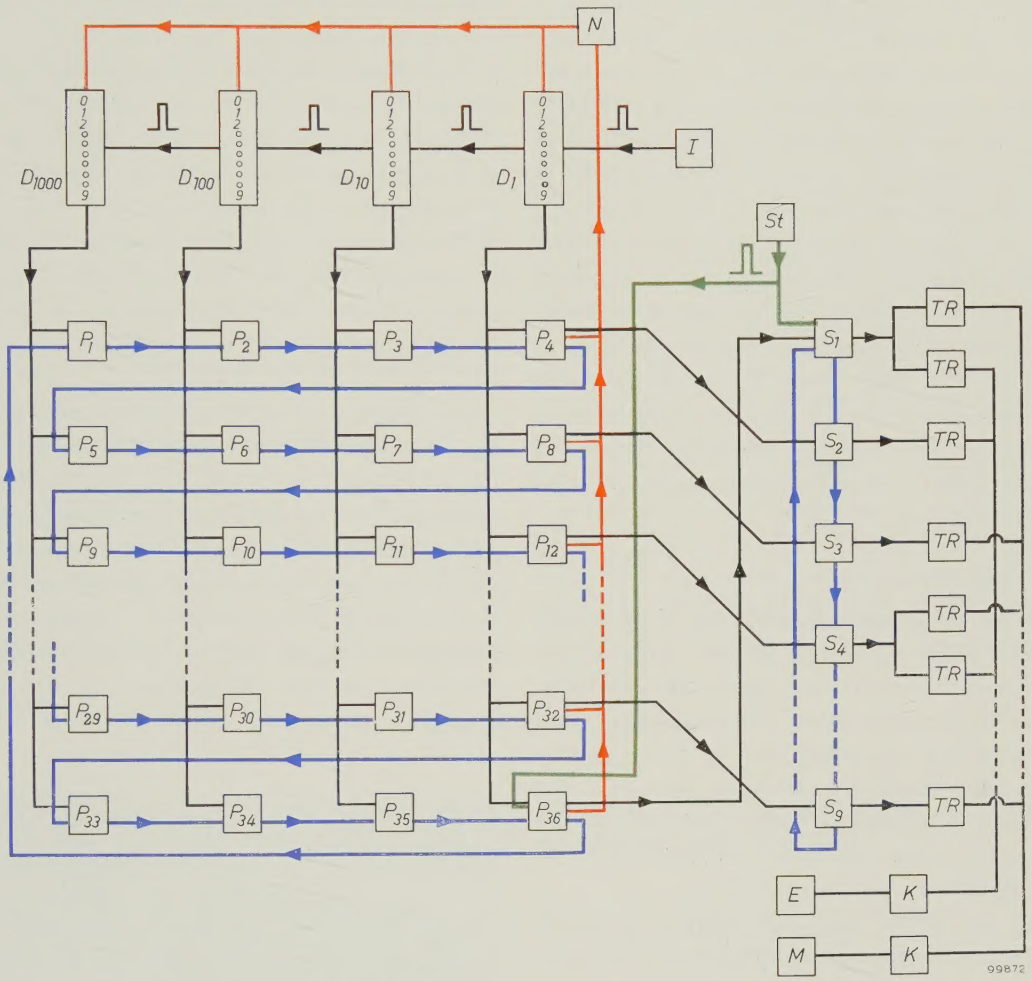

Fig. 8. Block diagram of the control circuit. D_1, D_{10}, D_{100}, D_{1000} decades of the counter. *I* pulse generator. *N* zero resetter. *St* starting circuit. P_1-P_{36} programmer tubes. S_1-S_9 switching tubes. *TR* Schmitt trigger circuits. *K* power transistors. *M* motor. *E* electromagnetic clutch. Black connections are those for the count pulses, firing voltages and switching voltages; blue connections are for the bias voltages; red connections are for the zero reset voltage; green connections are for the starting pulse.

sider the case in which 6501 pulses have to be counted for the first stage. P_1 will then normally fire at 6000, P_2 at 6500. For 6501, P_3 should fire simultaneously with P_2 and supply the bias to P_4, since that tube has to fire at the *next* count pulse. If the trigger of P_3 (with the corresponding switch set to position *0*) were connected to the cathode of tube *0* of the tens decade, however (as corresponds to other positions of the switch), P_3 would not fire at all. This is because after 6499 pulses it is *first* the unit decade of the counter that changes to zero and then the tens decade, and only then does the latter supply a pulse to the hundreds decade, changing it to 5. This fires P_2 and only then will P_3 be biased. P_3, however, can no longer fire, because tube *0* of the tens decade is already conducting and the ignition pulse is no longer available. In this case it is accordingly necessary to bypass P_3 in the circuit; P_4 must obtain its bias directly from P_2. It is therefore arranged that when a ten-position switch is in position *0*, the bias received from the preceding programmer tube is directly relayed to the next programmer tube.

The switching unit

Next to the programme tubes in fig. 8 are shown the switching tubes S_1-S_9, one for each stage of the winding process. These nine tubes are similarly arranged in ring configuration. The cathode of each tube is connected to either one or two Schmitt trigger circuits, which are triggered whenever the corresponding programmer tube ignites, thereby controlling the current to the winding motor and/or magnetic clutch via power transistors.

To start the whole winding process, a 300 V pulse is required. This pulse is obtained by discharging a capacitor across a resistor when a push-button is depressed. The pulse ignites S_1 and P_{36}. The two Schmitt circuits connected to S_1 are then triggered, energizing motor and magnet for the first stage (coiling). The cathode voltage of P_{36} has three effects: 1) zero-resetter N is activated; 2) P_1 is biased and the first number is now counted off as described above for the programmer unit; 3) the voltage is applied to the trigger electrode of S_1 (which is necessary at the end of the programme). Because S_1 is now conducting, S_2 is biased. The cathode of P_4 is connected to the trigger electrode of S_2. When the first number is reached, P_4 fires and S_2 fires immediately afterwards. This extinguishes S_1, and motor and magnet are cut out. The Schmitt circuit following S_2, however, is immediately triggered, thus directly energizing the magnet again. The magnetic clutch does not respond to this very short interruption of the current. The motor remains switched off, and winding is slowing down. P_4 has meanwhile also activated the zero-resetter and biased P_5, so that now the second number is counted off. Upon completion, P_8 ignites, so that S_3 (biased by S_2) fires: the third stage therefore commences (motor only switched on, forming straight section of filament). During the last stage, S_1 is biased and can therefore be ignited by P_{36}, enabling the programme to be repeated without interruption, i.e. to wind a second filament, and so on. During each stage the corresponding switching tube remains conducting, so that there is always visual indication of the stage in progress at any moment.

By means of the 36 ten-position switches the 9 numbers can be independently varied, which makes a highly flexible system.

Construction of the equipment

The major part of the circuit is accommodated in boxes of $40 \times 104 \times 117$ mm. Printed wiring is used for all component parts, and connections between containers are established by contact strips forming part of the printed wiring. The contact strips fit into special sockets arranged on a panel. Each decade is housed in its own container, together with two programmer tubes and the two corresponding digit switches (*fig. 9*). The position of the counter is indicated through the windows at the front. The

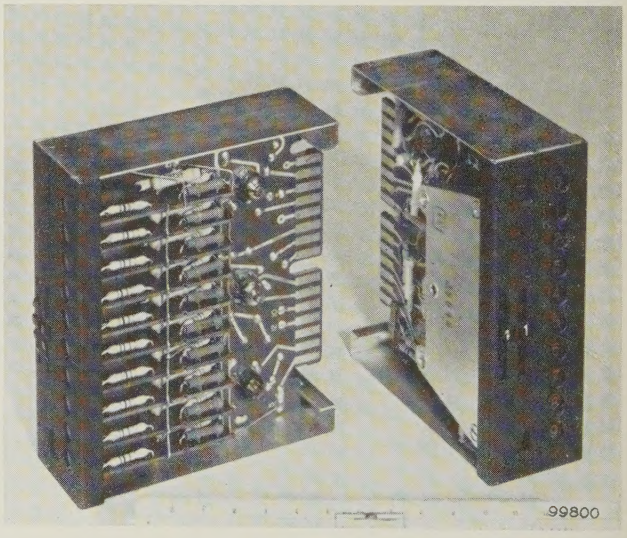

Fig. 9. Two views of a decade of the counting circuit; each decade chassis also houses two programmer tubes and their ten-position switches. If more than two stages are to be programmed (nine in the case described here), additional programmer tubes are available (for each decade). The numbered windows behind which the counting tubes are fitted can be seen on the front of the decade boxes. The tubes are painted black to prevent premature firing by incident light. The decade switches together with figures indicating their positions can also be distinguished.

digit switches can be manipulated from the front and their positions read. The remaining programmer tubes are accommodated in pairs or groups of four in further boxes, together with their switches, and may be independently connected up to a decade. The switching tubes are housed in a separate box. The auxiliary circuits, being likewise made with printed wiring, can be similarly incorporated into the circuit.

The equipment described here has possibilities beyond that of controlling a coil-winding machine. Generally speaking, it can be employed whenever some switching action has to follow a specified number of occurrences, as long as these occurrences can be translated into light or voltage pulses. As examples we mention the control of machine tools by counting the number of revolutions of drive shafts, and the counting and sorting of objects on belt conveyors.

Switching can also take place after specified time intervals. The circuit is then fed with pulses from a pulse generator with a known and constant frequency. This possibility has been used for coating bulbs with an internal mirror. This is done by vaporizing a piece of aluminium within the evacuated bulb, after which the aluminium vapour settles as a deposit on the wall. The times required for evacuating the bulb, for heating the aluminium and for cooling down, depends upon the type of bulb treated. With the apparatus described these times can be rapidly preselected and changed. For small runs, especially, the flexibility of the apparatus again shows up to advantage over mechanical control.

Summary. In various incandescent lamps, e.g. those for projectors, the filaments consist of coiled sections linked by sections of uncoiled wire. Filaments of this kind can be made on a filamentwinding machine by decoupling the winding head from the motor drive for a few specified periods. Motor and coupling must be energized in accordance with a preselected programme, according to the type of filament required. The machine was hitherto mechanically controlled by cams. An electronic control has now been designed for the same purpose. It has the advantage that for small runs, e.g. in developing new types, the dimensions of the filament produced can easily be varied. The control is operated by voltage pulses derived from the periodic interruption of a light beam by a perforated disc fitted to the motor spindle. The pulses are applied to a decade counter circuit incorporating cold cathode tubes, type Z 70 U, as switching elements. Upon reaching a preset number (set by a switch in each decade), corresponding to a given length of coil (number of revolutions of the motor), the counter controls a transistorized switching unit, which switches the currents through motor and magnetic coupling. In this way the various stages of the winding programme are successively completed. The control apparatus is in principle also applicable to other manufacturing processes, e.g. in which the preselected numbers correspond to time intervals. As an example an installation for the internal silvering of bulbs is mentioned.

ABSTRACTS OF RECENT SCIENTIFIC PUBLICATIONS BY THE STAFF OF N.V. PHILIPS' GLOEILAMPENFABRIEKEN

Reprints of these papers not marked with an asterisk * can be obtained free of charge upon application to Philips Electrical Ltd., Century House, Shaftesbury Avenue, London W.C. 2, where a limited number of reprints are available for distribution.

2698: P. B. Braun and J. L. Meijering: The copper-rich part of the copper-barium system (Rec. Trav. chim. Pays-Bas **78**, 71-74, 1959, No. 1).

The system Cu-Ba was examined up to 75% Ba by weight. At 675 °C there is a peritectic three-phase equilibrium Cu + liquid $\rightleftarrows$ $Cu_{13}Ba$. The compound $Cu_{13}Ba$ has KZn_{13} structure. At 550 °C there is a eutectic three-phase equilibrium liquid $\rightleftarrows$ $Cu_{13}Ba$ + Cu_xBa_y. Composition and structure of the latter could not be determined owing to experimental difficulties.

2699: W. Kwestroo: Spinel phase in the system MgO-Fe_2O_3-Al_2O_3 (J. inorg. nucl. Chem. **9**, 65-70, 1959, No. 1).

The three-component system MgO-Fe_2O_3-Al_2O_3 has been investigated at 1250 °C and at 1400 °C. The binary parts of this system, already described some twenty years ago, are reviewed and completed. The ternary diagram shows a broad spinel area: this area increases with increasing temperatures. The preparations do not contain Fe^{2+} ions, as was ascertained by analytical methods and by D.C. resistivity measurements. The resistivity has a fairly high value. The physical properties are roughly in agreement with the properties already found in systems investigated previously. Substituting Al^{3+} ions for Fe^{3+} ions in the spinel phase lowers the value of the magnetic saturation and the Curie temperature. An increasing amount of Fe_2O_3 in the spinel phase increases the magnetic saturation and the Curie temperature. Samples with the composition of a mineral called "hoegbomite" have been investigated and the possible structure of this mineral is discussed.

2700: J. Goorissen and F. Karstensen: Das Ziehen von Germanium-Einkristallen aus dem „schwimmenden Tiegel" (Z. Metallk. **50**, 46-50, 1959, No. 1). (Pulling germanium single crystals from a floating crucible; in German.)

Single crystals of germanium with a homogeneous impurity concentration can be prepared if enrichment or exhaustion of the impurity in the melt is prevented. This is made possible by means of the floating-crucible technique. In this technique a small crucible from which the crystal is pulled floats on the molten germanium in a larger outer crucible. Communication between both crucibles is made possible by means of a capillary allowing a continuous replacement of the solidified germanium. The theoretical yield of this technique is compared with that of the Czochralski method and of zone levelling. See also Philips tech. Rev. **21**, 193-195, 1959/60 (No. 7).

2701: H. J. G. Meyer: Theory of infrared absorption by conduction electrons in germanium (Phys. Chem. Solids **8**, 264-269, 1959).

It is shown that a theory of infrared absorption by conduction electrons which takes into account the structure of the conduction band and acoustical as well as optical intra-valley scattering can be developed without any serious approximation. In combination with an estimate of the possible influence of impurity scattering the theoretical results can be used for the determination of one of the acoustical and of the optical deformation potential constants. From available experimental data the approximate numerical value of the latter is determined. The general limits of validity of the theory are discussed.

2702: K. W. van Gelder: Fabricagebeheersing, I. Procesnauwkeurigheid en het stellen van toleranties (Sigma **5**, 15-19, 1959, No. 1). (Process control, I. Process accuracy and the specification of tolerances; in Dutch.)

First of two articles (see also **2719**) in which the author attempts to fuse the essentials of manufacturing processes (derived from analysis of such processes) with statistical concepts, and thus arrive at process control. This first article contains firstly a simple example of a process analysis (pressing and centreless grinding of plastic coil bobbins), which he uses to draw conclusions as regards the choice of tolerances. This is further considered in a second example. Finally, more complicated cases are dealt with in which so-called combined tolerances occur.

2703: G. H. Jonker: Analysis of the semiconducting properties of cobalt ferrite (Phys. Chem. Solids **9**, 165-175, 1959, No. 2).

From measurements of resistivity, activation energy, and Seebeck effect, an energy-level scheme is derived by which the semiconducting properties of $CoFe_2O_4$ can be described. These properties differ considerably from those of normal semiconductors, as the charge carriers are not free to move through the crystal lattice but jump from ion to ion.

2704: M. J. Sparnaay: On the additivity of London-Van der Waals forces (Physica **25**, 217-231, 1959, No. 3).

Calculations are given concerning the additivity of London-Van der Waals forces between two groups of atoms, the atoms being represented as isotropic harmonic oscillators. The results indicate that deviations of 10-30% from additivity can be obtained if only dipole-dipole interaction between oscillators of one group is assumed. The effect can be expected to be relatively large if the symmetry of the arrangements of the oscillators in the group is low, and it is dependent upon the relative spatial position of the groups.

2705: G. Diemer and P. Zalm: The role of exhaustion barriers in electroluminescent powders (Physica **25**, 232, 1959, No. 3).

Note concerning the apparent paradoxical effects of Mott-Schottky barriers in phosphor grains in an insulating medium. The explanation of the apparent paradox lies in the fact that electroluminescence occurs only in tiny localized spots where exhaustion barriers can indeed give rise to a local enhancement of the electric field.